The tri-snRNP specific protein FgSnu66 is functionally related to FgPrp4 kinase in *Fusarium graminearum*

Manli Sun[1], Yimei Zhang[1], Qinhu Wang[1], Chunlan Wu[1], Cong Jiang[1], and Jin-Rong Xu[1, 2*]

[1] State Key Laboratory of Crop Stress Biology for Arid Areas and NWAFU-Purdue Joint Research Center, College of Plant Protection, Northwest A&F University, Yangling, Shaanxi 712100, China.

[2] Department of Botany and Plant Pathology, Purdue University, West Lafayette, IN 47907, USA.

*** Corresponding author:** Jin-Rong Xu,

Department of Botany and Plant Pathology,

Purdue University,

West Lafayette, IN 47907, USA

Tel: 1-765-496-6918, email: jinrong@purdue.edu

Keywords: pre-mRNA splicing, tri-snRNP, Snu66, Hub1, Prp4, *Gibberella zeae,* spliceosome activation

Running title: Suppressor mutations in *FgSNU66*

This article has been accepted for publication and undergone full peer review but has not been through the copyediting, typesetting, pagination and proofreading process which may lead to differences between this version and the Version of Record. Please cite this article as an 'Accepted Article', doi: 10.1111/mmi.14005

SUMMARY

Deletion of Prp4, the only kinase among spliceosome components, is not lethal in *Fusarium graminearum* but *Fgprp4* mutants have severe growth defects and produced spontaneous suppressors. To identify novel suppressor mutations of *Fgprp4*, we sequenced the genome of suppressor S37 that was normal in growth but only partially recovered for intron splicing and identified a tandem duplication of 9-aa in the tri-snRNP component *FgSNU66*. Among the 19 additional suppressor strains found to have mutations in *FgSNU66* (out of 260 screened), five had the same 9-aa duplication event with S37 and another five had the R477H/C mutation. The rest had nonsense or G-to-D mutations in the C-terminal 27-aa (CT27) region of FgSnu66, which is absent in its yeast ortholog. Truncation of this C-terminal region reduced the interaction of FgSnu66 with FgHub1 but increased its interaction with FgPrp8 and FgPrp6. Five phosphorylation sites were identified in FgSnu66 by phosphoproteomic analysis and the T418A-S420A-S422A mutation was shown to reduce virulence. Overall, our results showed that mutations in *FgSNU66* can suppress deletion of *Fgprp4*, which has not been reported in other organisms, and the C-terminal tail of FgSnu66 plays a role in its interaction with key tri-snRNP components during spliceosome activation.

INTRODUCTION

The homothallic ascomycete *Fusarium graminearum* is one of the causal agents of Fusarium head blight (FHB), a devastating disease of wheat and barley (Bai & Shaner, 2004, Goswami & Kistler, 2004). Besides causing yield loss, infested grains often are contaminated with mycotoxins deoxynivalenol (DON) and zearalenone (Trail, 2009). As a potent inhibitor of protein synthesis in eukaryotic organisms, DON is also an important virulence factor in this pathogen (Desjardins, 2003). Unlike many other plant pathogenic fungi, ascospores produced on plant debris are the primary inoculum in *F. graminearum*, which is also a pathogen of corn and other small grains (Bai & Shaner, 1994, Bai & Shaner, 2004).

Like in other eukaryotic organisms, protein kinases play key roles in regulating growth and developmental process and responses to environmental stresses in fungi (Cohen, 2000). In a systematic functional characterization of protein kinase genes in *F. graminearum*, one of the mutants with severe growth defects was the *Fgprp4* deletion mutant (Wang *et al.*, 2011, Gao *et al.*, 2016). Although it is absent in the budding yeast *Saccharomyces cerevisiae*, a model for studying spliceosome and intron splicing, Prp4 is the only protein kinase among all the known spliceosome components (Kuhn & Käufer, 2003, Schneider *et al.*, 2010, Boesler *et al.*, 2015). In the fission yeast *Schizosaccharomyces pombe* and other eukaryotic organisms, the Prp4 kinase gene is essential for viability (Rosenberg *et al.*, 1991, Schneider *et al.*, 2010). In *F. graminearum*, the *Fgprp4* mutant was unstable and it spontaneously produced fast-growing suppressors (Gao *et al.*, 2016). Among the first 49 suppressors sequenced for 10 candidate

genes, suppressor mutations were identified in the *BRR2, PRP6, PRP8,* and *PRP31* orthologs (Gao *et al.*, 2016). In *S. pombe*, suppressor mutations of the temperature sensitive *prp4* also have been identified in these four key tri-snRNP components (Schmidt *et al.*, 1999, Bottner *et al.*, 2005).

Spliceosome is a dynamic complex responsible for intron splicing and proper gene expression in eukaryotic organisms (Will & Lührmann, 2011). It consists of five small nuclear ribonucleoprotein particles (snRNP) named U1, U2, U4, U5, and U6. The Prp4 kinase is involved in the activation of pre-catalytic B complex that is formed by the integration of pre-assembled U4/U6·U5 tri-snRNP into A complex consisting of pre-mRNA, U1 snRNP, and U2 snRNP. After being catalytically activated, U1 and U4 are disassociated along with changes in RNA-protein associations to form the B^{act} (activated B) complex. The B* complex catalyzes the first of the two sequential trans-esterification reactions involved in intron splicing (Will & Lührmann, 2011). Recently, the structure of tri-snRNP and activation of spliceosome have been characterized by cryo-EM studies in *S. cerevisiae, S. pombe,* and humans (Mozaffari-Jovin *et al.*, 2013, Nguyen *et al.*, 2015, Yan *et al.*, 2015, Agafonov *et al.*, 2016). Before catalytic activation of the spliceosome, RNA-binding and U4/U6 unwinding activities of Brr2 are blocked by the insertion of the C-terminal tail of Prp8 into its RNA-binding tunnel (Mozaffari-Jovin *et al.*, 2013). During activation, Brr2 undergoes a conformational change along with the rearrangement of Prp8 (Stevens *et al.*, 2001, Agafonov *et al.*, 2016).

Snu66 is a conserved component of the U4/U6·U5 tri-snRNP complex (Gottschalk *et al.*, 1999, Stevens & Abelson, 1999). Deletion of *SNU66* in *S. cerevisiae* is not lethal but results in

defects in the first step of splicing and cold-sensitivity (van Nues & Beggs, 2001). However, *snu66* is an essential gene in *S. pombe* and its overexpression inhibits the *hub1*^{ts} mutant (Wilkinson *et al.*, 2004). Hub1, an ubiquitin-like protein important for intron splicing and splice-site usage, binds to Snu66 at its Hub1-interacting domain (HIND) (Mishra *et al.*, 2011). In the yeast spliceosome, the N-terminal region of Snu66 forms a globular domain to interact with the endonuclease-like domain of Prp8 and N-terminal ratchet domain of Brr2 (Nguyen *et al.*, 2016). A long helix in the middle region of Snu66 wedges between the Prp8 Jab1/MPN and Brr2 N-terminal HLH domains (Nguyen *et al.*, 2016). The C-terminal region of Snu66 wraps around Brr2 and has extensive interactions with its C-terminal cassette, which is consistent with results from yeast two-hybrid and co-immunoprecipitation (co-IP) assays (van Nues & Beggs, 2001). In humans, hSnu66 is a tri-snRNP-specific protein that is essential for B complex formation *in vitro* (Makarova *et al.*, 2001). It plays a role in bridging the snRNP components of tri-snRNP (Liu *et al.*, 2006) by interacting with both U5-specific (e.g. Prp6, Brr2) and U4/U6-specific proteins.

To date, suppressor mutations of *prp4* have been reported only in the *BRR2, PRP6, PRP8,* and *PRP31* orthologs in *S. pombe*. In *F. graminearum*, among the 49 *Fgprp4* suppressor strains analyzed in a previous study (Gao *et al.*, 2016), nine had suppressor mutations in these four genes, but suppressor mutations in the rest remained to be identified. This study aimed to identify novel suppressor mutations of *Fgprp4* and characterize their roles in spliceosome activation. We used the whole genome sequencing approach to identify mutations in suppressor S37 that was partially recovered in intron splicing defects and pleiotropic phenotypes of *Fgprp4*.

A tandem duplication of RLKKIEDEK was identified in *FgSNU66* in suppressor S37 and confirmed to suppress *Fgprp4* mutant. Nineteen additional suppressors with mutations in *FgSNU66* were identified. Among them, five had the same 9 aa duplication with S37 and nine had either nonsense or G-to-D mutations in the C-terminal 27 aa (CT27) region of FgSnu66, which is absent in its yeast ortholog. In yeast two-hybrid assays, truncation of this C-terminal region reduced the interaction of FgSnu66 with FgHub1 but increased its interaction with FgPrp8 and FgPrp6. Taken together, our results showed that mutations in *FgSNU66* could suppress deletion of *FgPRP4*, which has not been reported in other organisms. Furthermore, we showed that the C-terminal tail of FgSnu66 likely plays a role in its interaction with key components of tri-snRNP in *F. graminearum*, which may be regulated by FgPrp4 kinase during spliceosome activation.

RESULTS

Suppressor S37 has a duplication of 9-amino acids in *FgSNU66*

The *Fgprp4* mutant had severe defects in growth but often produced fast-growing suppressors after incubation for 2 weeks (Wang *et al.*, 2011, Gao *et al.*, 2016). Among the first 49 randomly collected suppressor strains, nine had suppressor mutations in the *BRR2*, *PRP6*, *PRP8*, and *PRP31* orthologs. For the rest 40 suppressor strains, none of them had mutations in the 10

candidate genes sequenced (Gao *et al.*, 2016). To identify novel suppressor mutations, in this study we selected suppressor S37 (Table 1) for whole genome sequencing analysis because it had the same growth rate with the wild type strain and was normal in sexual reproduction.

Approximately 50X coverage of the genome sequence of S37 was generated by Illumina Hi-seq (Liu *et al.*, 2016). When aligned with the reference genome of the wild-type strain PH-1 (Cuomo *et al.*, 2007), four mutations were identified in the predicted genes (Table S1), including one synonymous mutation in FGSG_04322. Another mutation was a duplication of 27 nt (1864-1890) in FGSG_06279, a *SNU66* ortholog (Table S1), resulting a tandem duplication of nine amino acids (aa) residues (RLKKIEDEK) towards its C-terminal region (Fig. 1A). The other two mutations resulted in the K98R mis-sense and frameshift at L70 mutation, respectively, in the hypothetical genes FGSG_09392 and FGSG_05186 (Table S1) that had no orthologous genes in *S. cerevisiae*.

The 9 aa tandem duplication in *FgSNU66* is suppressive to the *Fgprp4* mutant

Because its ortholog is a tri-snRNP specific protein involved in intron splicing in yeast and humans, the mutation in FGSG_06279 (named *FgSNU66* in this study) was selected for verification for the suppressive effects. The *FgSNU66* fragment carrying the 9 aa duplication (described as 9aaD below) was amplified from suppressor strain S37 and used to generate the *in situ FgSNU66*^{9aaD} gene replacement construct (Fig. S1A) by the split-marker approach with the geneticin-resistance cassette (Gen^{R}) from pFL2 (Zhou *et al.*, 2011a). The resulting PCR products were co-transformed with the hygromycin-resistant *FgPRP4* knockout cassette (Wang

et al., 2011) into the wild-type strain PH-1. Transformants resistant to both hygromycin and geneticin were screened by PCR for the deletion of *FgPRP4* and replacement of endogenous *FgSNU66* with *FgSNU66*^{9aaD}. Similar to suppressor strain S37, the resulting *Fgprp4* *FgSNU66*^{9aaD} transformants were normal in growth rate and sexual reproduction (Fig. 1B) but defective in conidiation (Table 2) and plant infection in comparison with the wild type (Fig. 1C). Whereas the *Fgprp4* mutant was almost non-pathogenic, the average disease index of *Fgprp4* *FgSNU66*^{9aaD} transformants was 6.0 (Table 2), which was similar to that of suppressor strain S37 (6.4) but significantly lower than that of PH-1 (13.6). These results indicate that the 9 aa tandem duplication in *FgSNU66* was responsible for suppressing the growth but not plant infection defect of *Fgprp4* in S37.

To determine the effect of RLKKIEDEK duplication on FgSnu66 functions, we then transformed the *FgSNU66*^{9aaD} gene replacement construct (Fig. S1A) into the wild-type strain PH-1. After screening 47 geneticin-resistant transformants, 40 *FgSNU66*^{9aaD} mutants were identified. All the *FgSNU66*^{9aaD} mutants were normal in growth, sexual reproduction, and plant infection (Fig. S2). In comparison with PH-1, the *FgSNU66*^{9aaD} mutants had no obvious defects, indicating that the duplication of RLKKIEDEK may have no or only minor effect on its normal functions in the wild type when the FgPrp4 kinase is present.

Intron splicing defects of *Fgprp4* is partially recovered in suppressor S37

To further confirm the suppressive effect of *FgSNU66*^{9aaD} on *Fgprp4*, we conducted RNA-seq analysis with RNA isolated from aerial hyphae harvested from 9-day-old PDA cultures of PH-1,

Fgprp4 mutant, and suppressor strain S37. Consistent with the previous study, the level of retained introns (un-spliced introns) in *Fgprp4* was significantly higher than in PH-1 (Gao *et al.*, 2016). In comparison with *Fgprp4*, the intron retention level in strain S37 was significantly reduced (p<0.0001, t-test) (Fig. 2A). Approximately 55% of the introns with increased retention rate in *Fgprp4* were recovered to the normal level in S37. These results indicate that the 9 aa duplication in *FgSNU66* partially suppressed intron-splicing defects of *Fgprp4*. To verify this observation, we selected 4 introns that had increased splicing efficiency in suppressor S37 for RT-PCR analysis. All of them had lower intron retention levels in S37 than in *Fgprp4* (Fig. 2B), confirming that the intron splicing efficiency was partially recovered in suppressor S37, which may contribute to its phenotype suppression.

Nineteen additional suppressor strains have mutations in *FgSNU66*

Recently, 260 additional type I spontaneous suppressors of *Fgprp4* (Gao *et al.*, 2016) with faster growth rate and normal colony morphology were isolated (Gao *et al.*, 2018). After PCR amplification and sequencing analysis, mutations in *FgSNU66* were identified in 19 of them (Table 3). Five of them, including S92 and S221, had the same mutation with S37 in *FgSNU66* (Fig. 3D), further proving the suppressive effect of this 9 aa duplication on *Fgprp4*. Interestingly, except five suppressors with the R477H or R477C mutation, all the other suppressor strains had mutations in the C-terminal 46 aa region of *FgSNU66* (Fig. 3A). The distribution of these suppressor mutations indicates the importance of R477 residue and C-terminal region of FgSnu66 in *F. graminearum*.

Like S37, none of the suppressors with mutations in *FgSNU66* was fully recovered in virulence in infection assays with wheat heads (Fig. 3B) or corn silks (Fig. 3C). All of them grew faster than the *Fgprp4* mutant although they varied slightly in growth rate (Fig. 3D). Most of them, similar to S37, were normal in sexual reproduction but suppressors S60, S108, and S131 formed perithecia that were defective in ascospores formation (Fig. 3E). These results further showed that suppressor mutations in *FgSNU66* only partially rescued the defects of *Fgprp4*.

Non-sense mutation at R644 in *FgSNU66* partially suppresses the growth defect of *Fgprp4*

Because 9 of 20 suppressors have mutations in the C-terminal 24 aa region, we selected the R644* mutation identified in suppressor S131 for verification. The *FgSNU66*^{R644*} gene replacement construct (Gen^{R}) was generated by the split-marker approach (Fig. S1B) and co-transformed with the *FgPRP4* knockout cassette (Wang *et al.*, 2011) into protoplasts of PH-1. Transformants resistant to both hygromycin and geneticin were screened for deletion of *FgPRP4* and integration of *FgSNU66*^{R644*} and verified by sequencing analysis. Similar to suppressor S131, the *Fgprp4 FgSNU66*^{R644*} transformants grew slower than the wild type but faster than *Fgprp4* mutant (Fig. 3D). They also had similar defects with suppressor S131 in conidiation (Table 2), sexual reproduction (Fig. 3E), and infection of wheat heads (Fig. 3B) or corn silks (Fig. 3C). These results indicated that the non-sense mutation at R644 in *FgSNU66* was responsible for the partial phenotype recovery observed in suppressor S131.

The R477H mutation has no effect on the localization of FgSnu66 to the nucleus

To determine its subcellular localization, the *FgSNU66*-GFP fusion construct was generated by gap repair (Bruno *et al.*, 2004) and transformed into PH-1. The resulting *FgSNU66*-GFP fusion transformants (Table 1) were normal in growth, conidiation, and sexual reproduction. When examined by epifluorescence microscopy, GFP signals were observed in the nucleus in conidia and hyphae (Fig. 4A). The localization of FgSnu66-GFP to the nucleus was confirmed by staining with 4, 6-diamidino-2-phenylindole (DAPI). This observation is consistent with its function in the spliceosome and the localization of Snu66 in *S. cerevisiae* (Stevens *et al.*, 2001).

It has been reported that arginine methylation influences the localization of the oncoprotein splicing factor SF2/ASF to the nucleus and affects alternative splicing of its targets (Sinha *et al.*, 2010). To determine the effect of R477H mutation on its localization, the *FgSNU66*^{R477H}-GFP fusion construct was generated and transformed into PH-1. In the resulting transformants, GFP signals were still mainly observed in the nucleus (Fig. 4B), indicating that the R477H mutation had no obvious effect on the localization of FgSnu66. We also transformed the *FgSNU66*-GFP fusion construct into the *Fgprp4* mutant. In the resulting transformants, FgSnu66-GFP proteins also mainly localized to the nucleus (Fig. 4B), indicating that FgPrp4 kinase plays no direct role in the subcellular localization of FgSnu66 in *F. graminearum*.

Deletion of the C-terminal 27 aa of *FgSNU66* is suppressive to the *Fgprp4* mutant

Five suppressor strains had nonsense mutations that resulted in the truncation of the C-terminal

tail of *FgSNU66*. Sequence alignment showed that Snu66 of *S. pombe* is 27 aa shorter than FgSnu66 at the C-terminus (Fig. 3A). To determine the function of C-terminal 27 aa (CT27) of FgSnu66, we generated the *FgSNU66*$^{\Delta CT27}$ replacement construct (Fig. S1C) by the split-marker approach and co-transformed it with the *FgPRP4* knockout construct (Wang *et al.*, 2011) into PH-1. Transformants deleted of *FgPRP4* and CT27 of *FgSNU66* were identified by PCR and confirmed by sequencing analysis. The resulting *Fgprp4 FgSNU66*$^{\Delta CT27}$ transformants (Table 1) were partially recovered in the defects of *Fgprp4* mutant in growth (Fig. 5A), sexual reproduction (Fig. 5B), and plant infection (Fig. 5C). In infection assays with wheat heads, the disease index of the *Fgprp4 FgSNU66*$^{\Delta CT27}$ transformants was 7.0 (Table 2), which was less than 13.6 of PH-1 but the *Fgprp4* mutant was almost non-pathogenic (Gao *et al.*, 2016). These results suggested that, like the R644* mutation, deletion of CT27 in *FgSNU66* suppresses the defects of *Fgprp4*.

FgSNU66* and *FgHUB1* are essential genes in *F. graminearum

Whereas *snu66* (649 aa) is an essential gene in *S. pombe*, *SNU66* (587 aa) is dispensable for growth in *S. cerevisiae*. The identities of FgSnu66 with SpSnu66 and ScSnu66 were 26.5% and 19.1%, respectively. To determine whether it is an essential gene in *F. graminearum*, we generated the *FgSNU66* gene replacement construct by the split-marker approach (Fig. S3) and transformed it into PH-1. Over 400 hygromycin-resistant transformants from 10 independent transformations were isolated but none of them were *Fgsnu66* deletion mutants, indicating that *FgSNU66* is likely an essential gene in *F. graminearum*.

In *S. cerevisiae* and humans, Snu66 physically interacts with Hub1 via its HIND domain at the N-terminus. Like *snu66*, *hub1* is viable in *S. cerevisiae* but lethal in *S. pombe* (Dittmar *et al.*, 2002, Lüders *et al.*, 2003, Wilkinson *et al.*, 2004, Yashiroda & Tanaka, 2004). We also attempted to delete *FgHUB1* (FGSG_09442) by gene replacement (Fig. S3) but failed to identify *Fghub1* mutants after screening over 100 hygromycin-resistant transformants. It is likely that *FgHUB1* is also an essential gene in *F. graminearum*.

No interaction is detected between FgSnu66^{CT50} and FgSnu66^{N596}

One possible function of the C-terminal tail is to interact with other parts of FgSnu66. To test this hypothesis, we generated the *FgSNU66*^{CT50} (C-terminal 50 aa)-3xFLAG and *FgSNU66*^{N596} (truncated of CT50)-GFP constructs and transformed them into PH-1. The C-terminal 50 aa region was used in this experiment because 27 aa may be too short for co-immunoprecipitation (co-IP) assays. In total proteins isolated from the resulting transformants, both FgSnu66^{CT50}-3xFLAG and FgSnu66$^{\Delta CT50}$-GFP bands were detectable. However, the FgSnu66^{CT50}-3xFLAG band was not detected in proteins eluted from anti-GFP beads (Fig. S4). These results indicated that CT50 of FgSnu66 might not interact with its N-terminal region.

CT24 of FgSnu66 is inhibitory to its interaction with FgPrp8 and FgPrp6

As a U5 snRNP protein located at the heart of the catalytic core of spliceosome, Prp8 is a major scaffolding protein that interacts with Brr2 and Snu114 to form a salt-stable complex (Galej *et al.*, 2013, Nguyen *et al.*, 2015). Based on the two regions of yeast Snu66 that interact with Prp8

(Nguyen *et al.*, 2016), we generated the prey constructs of FgPrp8$^{1213\text{-}1789}$ containing the Thumb/X and endonuclease domains and FgPrp8$^{2101\text{-}2370}$ containing the Jab1/MPN domain. In yeast two-hybrid assays, both of them weakly interacted with FgSnu66$^{\Delta CT24}$ (suppressor mutation in S292) but not with FgSnu66^{WT} (Fig. 6A), indicating that the C-terminal region of FgSnu66 may be inhibitory to its interaction with FgPrp8.

As a component of tri-snRNP, Prp6 is phosphorylated during B-complex formation by Prp4 kinase (Schneider *et al.*, 2010). In yeast two-hybrid assays, FgPrp6 interacted with FgSnu66$^{\Delta CT24}$ but not with FgSnu66^{WT} (Fig. 6A). These results indicated that the C-terminal region of FgSnu66 plays a negative role in its interaction with FgPrp6. Quantitative assays for LacZ activities also showed that deletion of the CT24 region increased the interaction of FgSnu66 with FgPrp8 and FgPrp6 (Fig. 6B). Therefore, the C-terminal tail of FgSnu66 may be inhibitory to its interactions with FgPrp8 and FgPrp6 in *F. graminearum*.

Because the C-terminal region of Snu66 is known to interact with the Brr2 C-terminal cassette in *S. cerevisiae* (van Nues & Beggs, 2001), we also generate the prey constructs of FgBrr2N (1-872 aa) and FgBrr2C (1285-2206 aa). Unfortunately, both FgSnu66^{WT} and FgSnu66$^{\Delta CT24}$ had no detectable interactions with FgBrr2N or FgBrr2C in yeast two-hybrid assays (Fig. S5). In comparison with yeast Snu66, FgSnu66 has a longer C-terminal tail, which may interfere with its interaction with FgBrr2.

CT24 of FgSnu66 plays a positive role in its interaction with FgHub1

Hub1 is an evolutionally conserved ubiquitin-like modifier (UBL) that is involved in mRNA

splicing via its specific interaction with Snu66 (Mishra *et al.*, 2011). To test its interaction with FgSnu66, we generated the prey construct of FgHub1. Yeast transformants expressing the FgSnu66 bait and FgHub1 prey constructs grew on SD-Trp-Leu-His plates (Fig. 6A) and had β-galactosidase activities (Fig. 6B), indicating that they directly interacted with each other. FgSnu66$^{\Delta CT24}$ also interacted with FgHub1 although their interaction appeared to be weaker than the FgSnu66-FgHub1 interaction based on growth on SD-His plates (Fig. 6A) or LacZ activities (Fig. 6B). These results indicate that deletion of the C-terminal region of FgSnu66 weakens its interaction with FgHub1.

Phosphorylation of FgSnu66 at T418, S420, and S422 is likely important for its functions

To identify its phosphorylation sites, we generated the *FgSNU66*-3xFLAG fusion construct and transformed it into PH-1. Total proteins isolated from the *FgSNU66*-3xFLAG transformants were incubated with anti-FLAG beads. Proteins eluted from anti-FLAG beads were treated with trypsin and enriched for phosphopeptides with PolyMac as described (Iliuk *et al.*, 2010). The resulting phosphopeptides were analyzed by MALDI-TOF/TOF MS (Gao *et al.*, 2016). In total, we identified 160 phosphopeptides derived from 91 *F. graminearum* proteins (Table S2). Phosphorylation of FgSnu66 was detected at T418, S420, S422, T445, and S446 (Fig. 7A). All of these putative phosphorylation sites are in the middle region of FgSnu66 that is not well conserved among its orthologs.

To determine the roles of these putative phosphorylation sites in FgSnu66, we generated the *FgSNU66*$^{T418A\ S420A\ S422A}$-GFP and *FgSNU66*$^{T445A\ S446A}$-GFP constructs with the Gen^{R} marker

and co-transformed them with the *FdgSNU66* knockout construct (Hyg^R) into PH-1. Transformants resistant to both geneticin and hygromycin were screened by PCR for mutants that were deleted of endogenous *FgSNU66* but expressing the GFP fusion of mutant *FgSNU66* alleles. In total, three *FgSNU66*$^{T418A\ S420A\ S422A}$-GFP and three *FgSNU66*$^{T445A\ S446A}$-GFP transformants (Table 1) were confirmed to be deleted of endogenous *FgSNU66*. None of these *Fgsnu66 FgSNU66*$^{T418A\ S420A\ S422A}$ and *Fgsnu66 FgSNU66*$^{T445A\ S446A}$ strains had any defects in growth (Fig. 7B) and sexual reproduction (Fig. 7C). In infection assays with wheat coleoptiles, the *Fgsnu66 FgSNU66*$^{T418A\ S420A\ S422A}$ strains had no obvious defects but the *Fgsnu66 FgSNU66*$^{T418A\ S420A\ S422A}$ strains were significantly reduced in virulence (Fig. 7D). Similar results were obtained in infection assays with corn silks (Fig. 7D). These results indicated that phosphorylation of FgSnu66 at T418, S420, and S422 may be important for plant infection in *F. graminearum*.

DISCUSSION

Snu66 is a component of the U4/U6·U5 tri-snRNP involved in pre-mRNA splicing (Stevens & Abelson, 1999) and maturation of pre-5S rRNA (Li *et al.*, 2009). In humans, hSnu66 is essential for B complex formation *in vitro*. In this study, mutations in *FgSNU66* were found to partially suppress the defects of *Fgprp4* mutant. Prp4 is the only kinase among the spliceosome components that is absent in *S. cerevisiae* but essential in *S. pombe* (Schneider *et al.*, 2010). In *S. cerevisiae*, deletion of *SNU66* is not lethal but the *snu66* mutant was defective in pre-mRNA splicing (Stevens *et al.*, 2001, Wilkinson *et al.*, 2004). In *F. graminearum*, *FgSNU66* appears to be an essential gene, which is similar to *snu66* in *S. pombe* (Wilkinson *et al.*, 2004). *F. graminearum,* like *S. pombe*, has many more introns than *S. cerevisiae*, which may be related to the importance of Snu66 and Prp4 orthologs for its viability. It is likely that the *SNU66* orthologs are also essential in other filamentous ascomycetes. In *N. crassa*, mutants deleted of NCU11222, the *SNU66* ortholog, were not generated in the systematic gene knockout project (Colot *et al.*, 2006).

Interestingly, 19 of the randomly collected 260 spontaneous suppressor strains of the *Fgprp4* mutant (7.3%) had mutations in *FgSNU66*. The high frequency of suppressor mutations in this gene indicated that FgSnu66 is functionally related to FgPrp4 or FgPrp4 plays a critical role in regulating FgSnu66 functions in *F. graminearum*. Suppressor mutations of *prp4* in Brr2, Prp31, Prp6, and Prp8, key components of the tri-snRNP components have been reported in *S. pombe* (Bottner *et al.*, 2005, Schmidt *et al.*, 1999) and *F. graminearum* (Gao *et al.*,

2016). However, mutations in Snu66 have not been reported to suppress *prp4* mutant in *S. pombe* or any other organisms. In *S. cerevisiae* that lacks Prp4 kinase, mutations in *SNU66* are shown to affect its interaction with Hub1. Synthetic lethality of Δ*snu66 prp8** can be rescued by the expression of wild-type *SNU66* but not $SNU66^{RR\text{-}AA}$ (changing R16 and R47 in the HIND domain to A) or $SNU66^{\Delta HIND}$ (Mishra *et al.*, 2011). In humans, the R127A mutation in the HIND domain or deletion of the HIND domain in hSnu66 also affects its interaction with hHub1 (Mishra *et al.*, 2011). However, none of the suppressor mutations identified in this study were in the HIND domain or at the N-terminal region of FgSnu66 containing the HIND domain. In fact, most of the suppressor mutations were in its C-terminal end in *F. graminearum*.

We noticed that the 20 suppressor strains with mutations in *FgSNU66* were not identical in their phenotypes. One explanation is that different suppressor mutations may differ in their effects on FgSnu66 functions or intron retention levels. The observation that the tandem 9 aa duplication but not R644* mutation in *FgSNU66* fully recovered the defects of *Fgprp4* in growth and sexual reproduction supported this hypothesis. Nevertheless, these spontaneous suppressor strains likely had other random mutations in their genomes. In some of the suppressor strains, mutations in other un-related genes may contribute to some of the phenotypes observed. In suppressor strain S37, although duplication of the 9 aa in *FgSNU66* was shown to be responsible for suppressing *FgPRP4* deletion, three other genes had mutations in their ORFs. Whereas the mutation in FGSG_04322 was synonymous, the K98 to R mutation in FGSG_09392 and insertion of a C at 97 aa in FGSG_05186 may affect their functions. Both FGSG_05186 and FGSG_09392 encode hypothetical proteins that lack distinct homologs in the budding yeast but

are conserved in filamentous ascomycetes. Their functions in *F. graminearum* remain to be characterized.

The same 9 aa (27-bp) duplication event observed in S37 also occurred in five other suppressors, which accounted for over 33% (6/20) of independent suppressor mutations in *FgSNU66*. Although it is not clear why spontaneous mutation occurred at such a high frequency at this site ('hot spot'), this duplicated 27-bp sequence is flanked by the GAGAAGCG sequences (Fig. S6). Unequal crossing-over may occur at a relatively high frequency between these duplicated sequences and result in the duplication of these 9 aa (Fig. S6) in *F. graminearum*. The other hot spot for suppressor mutations in *FgSNU66* is R477 because five suppressors had the R477H or R477C mutation. Sequences alignment showed that R477 is conserved in its orthologs from other filamentous fungi. Because *FgSNU66* is an essential gene, one possible explanation is that mutation at R477 had a less detrimental effect on FgSnu66 function but could effectively bypass the absence of FgPrp4 kinase in *F. graminearum*. Indeed, suppressor strains with mutations at R477, like suppressors with the 9 aa duplication, grew as fast as the wild type and were normal in sexual or asexual reproduction.

In comparison with yeast Snu66, FgSnu66 has an extra 27 aa residues at the C-terminus that are conserved in Snu66 orthologs from filamentous ascomycetes. Interestingly, nine suppressor strains had missense or nonsense mutations in this C-terminal region, including the Q623*, G626D, Q632*, G642D, and R644* mutations. The tandem duplication of 9 aa observed in six other suppressors occurs only 12 aa upstream from this CT27 region, indicating its importance for FgSnu66 functions. The G to D mutations at G626 and G642 drastically

changed the amino acid property and both G626 and G642 are well conserved in the Snu66 orthologs from filamentous ascomycetes. For the nonsense mutations, all of them resulted in the truncation of the C-terminal tail of FgSnu66. All these suppressor mutations in the C-terminal region may affect the role of FgPrp4 in B-complex activation and intron splicing efficiency. RNA-seq analysis showed that the 9aaD suppressor mutation rescued the intron splicing efficiency for over 50% of the genes affected in the *Fgprp4* mutant. The tandem duplication of RLKKIEDEK that is enriched for lysine and alkaline residues may affect the folding of FgSnu66 or its interaction with other tri-snRNP proteins to bypass the requirement of FgPrp4 (Gao *et al.*, 2016).

In yeast, the N-terminal region of Snu66 (5-560 aa) forms a globular domain that interacts with Prp8 and Brr2 in the head domain of the U4/U6·U5 tri-snRNP but its C-terminal region (561-587 aa) was not modeled (Nguyen *et al.*, 2016). Intriguingly, their global classification approach showed 'open' and 'closed' conformations of the head and foot domains (Nguyen *et al.*, 2016). The globular domain of Snu66 interacts with the N-terminal domain of Prp8 in the 'closed' conformation, which interacts with Snu114 (Nguyen *et al.*, 2016). Except the R477H/C mutations, all the other 15 suppressor mutations occur in the C-terminal region of FgSnu66 that could not be predicted for its interacting partners in tri-snRNP based on the yeast tri-snRNP structure. In yeast two-hybrid assays, deletion of CT27 increased the interaction of FgSnu66 with FgPrp6 and FgPrp8 but decreased its interaction with FgHub1. Therefore, the CT27 of FgSnu66 likely plays an important role in its interaction with other tri-snRNP proteins, which may be related to their functions and relationship with Prp4 kinase in the spliceosome.

However, although we failed to detect the interaction between FgSnu66^{CT50} and FgSnu66^{N596}, it remains possible that the C-terminal region interacts with the other parts of FgSnu66 because the lack of NLS in CT50 may affect its subcellular localization and CT50 may be too short for proper folding.

Although yeast Snu66 has two, its orthologs from *S. pombe* and vertebrates have only one Hub1-interacting domain (HIND). The role of Hub1 in intron splicing is directly related to its binding with Snu66 via its HIND domain and Snu66 is the only HIND-containing spliceosome components in *S. pombe* and humans. In *F. graminearum*, FgSnu66 also is the only spliceosome protein with a HIND domain. Interestingly, the Prp38 but not Snu66 ortholog in *Arabidopsis* has the C-terminal HIND domain that is responsible for bringing AtHub1 to the spliceosome (Mishra *et al.*, 2011). Therefore, the Hub1-HIND interaction is conserved in eukaryotes and the position of HIND is not crucial for functions. Like Snu66 in *S. pombe*, FgSnu66 has an N-terminal HIND and it strongly interacted with FgHub1 in yeast two-hybrid assays. However, truncation of CT24 reduced the interaction of FgSnu66 with FgHub1, indicating a positive role of this C-terminal region in their interaction. In *S. cerevisiae*, the *hub1* and *snu66* mutants are viable and have only minor phenotypes under normal growth conditions (Dittmar *et al.*, 2002). In contrast, both *FgHUB1* and *FgSNU66* appear to be essential genes in *F. graminearum*, which is similar to *S. pombe*. (Wilkinson *et al.*, 2004, Yashiroda & Tanaka, 2004). It will be important to further characterize the role of FgHub1 and its interaction with FgSnu66 in spliceosome activation and intron splicing in *F. graminearum*.

Overall, our results showed that mutations in *FgSNU66* could suppress the *Fgprp4*

mutant, which has not been reported in any other eukaryotic organisms with the Prp4 kinase. The C-terminal tail of FgSnu66 likely is involved in regulating its interaction with other tri-snRNP components during spliceosome activation (Fig. 8). Suppressor mutations identified in this study may have similar effects on FgSnu66 functions to its phosphorylation by the FgPrp4 kinase in *F. graminearum*.

CONFLICT OF INTEREST

The authors declare that no conflict of interest exists.

ACKNOWLEGEMENTS

We thank Drs. Huiquan Liu and Chenfang Wang for fruitful discussions. We also thank Dr. Xuli Gao, Chaohui Li, and Xiaoping Li for assistance with yeast two-hybrid assays. This work was supported by grants from the US Wheat Barley Scab Initiative to JX and Northwest A&F University Young Talent Program to CJ.

EXPERIMENTAL PROCEDURES

Culture conditions and phenotype assays: The wild-type strain PH-1, suppressors, and all the transformants generated in this study were routinely cultured on potato dextrose agar (PDA) at 25^{o}C. Colony morphology, growth rate, conidiation, and sexual reproduction were assayed as described (Wang *et al.*, 2011). Protoplasts prepared from 12 h germlings were used for polyethylene glycol (PEG)-mediated transformation with hygromycin B (CalBiochem, La Jolla, CA, USA) and geneticin (Sigma-Aldrich, St. Louis, MO, USA) added to the final concentration of 300 μg ml^{-1} and 400 μg ml^{-1}, respectively, for selection (Hou *et al.*, 2002). Infection assays with corn silks, wheat heads, and wheat coleoptiles were assayed as described (Liu *et al.*, 2015, Yin *et al.*, 2018) .

Whole genome sequencing analysis with S37 and identification of mutations in *FgSNU66*: To identify mutations in suppressor S37, genomic DNA isolated from 12 h germlings were sequenced with the Illumina platform at Novogene (Beijing, China) to 50x coverage with pair-end libraries. The sequence reads were mapped onto the reference genome of strain PH-1 with Bowtie 2.23. Mutation sites were identified by SAMtools with the default parameters. Annotation of the mutation sites was performed with Variant Effect Predictor (VEP). To identify mutations in *FgSNU66*, its coding region was amplified from 260 additional suppressors of *Fgprp4* and sequenced.

RNA-seq analysis: Vegetative hyphae were harvested from 9-day-old PDA cultures and used for RNA isolation as described (Gao *et al.*, 2016). RNA-seq libraries were prepared and sequenced with Illumina HiSeq 2500 with the paired-end 2×150 bp model as described (Liu *et al.*, 2016). For each sample, at least 25 Mb high-quality reads were obtained. The resulting RNA-seq reads were mapped onto the reference genome of PH-1 by HISAT2. To filter out weakly expressed genes, only genes with a minimum expression level of 1 count per million were included in the analysis. The intron retention level was defined as the number of reads that aligned to the predicted intron divided by the number of reads aligned to the corresponding transcript (Gao *et al.*, 2016). RNA-seq data were deposited in the NCBI Sequence Read Archive database under accession numbers SRP149644 and SRP062439. Primers used for RT-PCR verification of selected introns were listed in Table S3.

Generation of *Fgprp4* transformants expressing the *FgSNU66*^{9aaD}, *FgSNU66*^{R644*}, or *FgSNU66*$^{\Delta CT27}$ allele: To generate the *Fgprp4 FgSNU66*^{9aaD} transformants, a 0.8-kb fragment containing the 9 aa tandem duplication and a 0.7-kb downstream fragment of *FgSNU66* (Fig. S1A) were amplified from suppressor S37 with primers listed in Table S3. After fusing with the geneticin resistance (Gen^{R}) marker amplified from plasmid pFL2 (Zhou *et al.*, 2011a) by overlapping PCR, the resulting PCR products were co-transformed with the *FgPRP4* gene replacement cassette (Wang *et al.*, 2011) into protoplasts of PH-1. Transformants resistant to both hygromycin and geneticin were screened by PCR for the deletion of *FgPRP4* and confirmed by sequencing analysis for the replacement of *FgSNU66* with the *FgSNU66*^{9aaD} mutant allele. The same split-marker approach was used to generate the *Fgprp4 FgSNU66*^{R644*} (Fig. S1B) and *Fgprp4 FgSNU66*$^{\Delta CT27}$ mutants (Fig. S1C).

To determine the effect of RLKKIEDEK duplication on FgSnu66 functions, we also transformed the *FgSNU66*^{9aaD} gene replacement fragments (Fig. S1A) into the wild-type strain PH-1. Geneticin-resistant transformants were screened by PCR and verified by sequencing analysis for the replacement of the endogenous *FgSNU66* allele with the *FgSNU66*^{9aaD} construct.

Generation of the *FgSNU66* and *FgHUB1* knockout constructs: The split-marker approach was used to generate the *FgSNU66* gene replacement constructs (Fig. S3A). In brief, the 0.7-kb upstream and 0.7-kb downstream fragments of *FgSNU66* were amplified with primer pairs 79-1F/79-2R and 79-3F/79-4R (Table S3), respectively, and fused with the *hph* cassette by overlapping PCR. The resulting PCR fragments were transformed into protoplasts of PH-1 and

hygromycin-resistant transformants were screened for the deletion of *FgSNU66* and integration of *hph* by PCR. Similar approaches were used to generate the *FgHUB1* gene replacement construct (Fig. S3B). After repeated tries, we failed to identify any *Fgsnu66* or *Fghub1* deletion mutant.

Identification of phosphorylation sites in FgSnu66: The *FgSNU66*-3xFLAG construct was generated by the yeast gap repair approach as described (Zhou *et al.*, 2011a). The resulting fusion construct rescued from Trp^+ yeast transformants was transformed into protoplasts of PH-1 and suppressor strain S47 of *Fgprp4*. Geneticin-resistant transformants were verified by PCR and confirmed for the expression of FgSnu66-3xFLAG by western blot analysis. Total proteins isolated from the *FgSNU66*-3xFLAG transformant were incubated with anti-FLAG M2 beads (Sigma) as described (Liu *et al.*, 2011) . Proteins eluted from anti-FLAG beads were digested with proteomics grade trypsin (Sigma) and enriched for phosphopeptides with the polymer-based metal ion affinity capture (PolyMAC) method (Iliuk *et al.*, 2010). The resulting phosphopeptides were analyzed with an ABI 4800 MALDI-TOF/TOF mass spectrometer. Proteome Discoverer (version 1.0; Thermo Fisher Scientific) was used to identify peptide sequences and phosphorylation sites as described (Iliuk *et al.*, 2010).

Yeast two-hybrid assays: For yeast two-hybrid assays, fragments of *FgPRP8*, *FgPRP6*, *FgHUB1*, and *FgBRR2* were amplified with primers listed in table S3 from the first-strand cDNA of PH-1 and cloned into the pGADT7 vector of the Matchmaker yeast (Clontech, Mountain View,

CA, USA). Similar strategies were used to generate the bait constructs of the wild-type and mutant *FgSNU66* alleles. The resulting bait and prey vectors were confirmed by sequencing analysis and transformed in pairs into yeast strain AH109 (Clontech). The Leu^+ Trp^+ transformants were isolated and assayed for growth on SD-Trp-Leu-His medium as described (Zhou *et al.*, 2011b). The positive and negative controls were from the Matchmaker library construction kit (Clontech). LacZ activities were quantitatively assayed with ortho-nitrophenyl-β-D-galactopyranoside (ONPG) as the substrate.

Generation of the *FgSNU66*$^{T418A\ S420A\ S422A}$- and *FgSNU66*$^{T445A\ S446A}$-GFP transformants: To introduce the T418A, S420A, and S422A mutations, the N-terminal fragment (containing 1-422 aa) and C-terminal (containing 418-646 aa) fragments of *FgSNU66* were amplified with primers listed in Table S3 and fused together by overlapping PCR. The overlapping PCR primers carried the nucleotide changes associated with the T418A, S420A, and S422A mutations. Products amplified by overlapping PCR were then co-transformed into yeast strain XK1-25 with *Xho*I-digested pFL2 (Gen^R) to generate the *FgSNU66*$^{T418A\ S420A\ S422A}$-GFP fusion construct by gap repair (Zhou *et al.*, 2011a). Similar strategies were used to generate the *FgSNU66*$^{T445A\ S446A}$-GFP construct. The resulting mutant alleles were confirmed by sequencing analysis and co-transformed into PH-1 with the *FgSNU66* gene replacement construct described above. Transformants resistant to both geneticin and hygromycin were screened by PCR for *FgSNU66* deletion and examined for GFP signals by epifluorescence microscopy.

Co-IP assays for the interaction between FgSnu66^{CT50} and FgSnu66^{N596}: The FgSnu66^{CT50}-3xFLAG and FgSnu66^{N596}-GFP fusion constructs were generated by the yeast gap repair approach (Zhou *et al.*, 2011a) and co-transformed into the wild-type strain PH-1. Total proteins were isolated from transformants expressing both FgSnu66^{CT50}-3xFLAG and FgSnu66^{N596}-GFP constructs and incubated with anti-GFP beads (Sigma-Aldrich, St. Louis, MO) as described (Hou *et al.*, 2015, Zhang *et al.*, 2017). Western blots of total proteins and proteins eluted from anti-GFP beads were detected with the anti-GFP (Roche, USA) and anti-FLAG (Sigma-Aldrich, USA) antibodies as described (Liu *et al.*, 2015).

TABLES AND FIGURE LEGENDS

Table 1. The wild type and transformants of *Fusarium graminearum* used in this study

Strain	Brief description	Reference
PH-1	Wild-type	(Cuomo *et al.*, 2007)
FP1	*Fgprp4* deletion mutant of PH-1	(Wang *et al.*, 2011)
S37	Spontaneous suppressor mutant of FP1	(Gao *et al.*, 2016)
T37	*Fgprp4 FgSNU66*^{9aaD} transformant	This study
9D08	*FgSNU66*^{9aaD} transformant of PH-1	This study
9D10	*FgSNU66*^{9aaD} transformant of PH-1	This study
S60, S92, S103, S108, S114, S121, S128, S131, S164, S166, S168, S170, S176, S203, S219, S221, S239, S272, S292	Spontaneous suppressor mutants of FP1	(Gao *et al.*, 2018)
T131	*Fgprp4 FgSNU66*^{R644*} transformant	This study
SG-1, SG-2, SG-3	*FgSNU66*-GFP transformants of PH-1	This study
RH-1, RH-2, RH-3	*FgSNU66*^{R477H}-GFP transformants of PH-1	This study
PRH-1, PRH-2, PRH-3	*Fgprp4 FgSNU66*^{R477H}-GFP transformants	This study
ΔCT27	*Fgprp4 FgSNU66*$^{\Delta CT27}$ transformant	This study
NC-1	*FgSNU66*^{N596}-GFP & *FgSNU66*^{CT50}-3xFLAG transformant of PH-1	This study
TSS-1, TSS-2, TSS-3	*FgSNU66*$^{T418A\ S420A\ S422A}$-GFP transformants of *Fgsnu66*	This study
TS-2, TS-4, TS-5	*FgSNU66*$^{T445A\ S446A}$-GFP transformants of *Fgsnu66*	This study

Table 2. Growth rate, conidiation, and virulence of *FgSNU66* mutants

Strain	Growth rate (mm/day)[a]	Conidiation (10^5 spores/ml)[b]	Disease Index[c]
PH-1 (wt)	22.1±0.1^{A}	14.6±1.7^{A}	13.6±1.8^{A}
S37 (suppressor)	22.3±0.1^{A}	12.6±0.9^{B}	6.4±1.4^{B}
T37 (*Fgprp4 FgSNU66*^{9aaD})	21.9±0.1^{A}	12.3±0.6^{B}	6.0±0.9^{B}
S131 (suppressor)	19.0±0.4^{B}	14.8±1.6^{A}	6.8±1.1^{B}
T131 (*Fgprp4 FgSNU66*^{R644*})	18.6±0.1^{B}	14.9±2.0^{A}	6.6±1.5^{B}
T27 (*Fgprp4 FgSNU66*$^{\Delta CT27}$)	18.8±0.1^{B}	9.7±2.1^{C}	7.0±1.0^{B}

[a] Average daily extension in colony diameter on PDA plates.

[b] Conidiation in 5-day-old CMC cultures.

[c] The number of diseased spikelets on each inoculated wheat heads at 14 dpi.

Mean and standard deviation were calculated with results from at least three replicates. Data were analyzed with Duncan's pair-wise comparison. Different letters mark significant differences (P= 0.05)

Table 3. Suppressor strains with mutations in *FgSNU66*

Suppressor strain	Mutation	Amino acid change
S37, S92, S121, S128, S219, S221	Duplication of CGTCTCAAGAAGAT CGAGGACGAGAAG (1864-1890 nt)	Tandem duplication of RLKKIEDEK (603-611)
S60, S203	CG^{1487}C to CAC	R477 to H
S103, S164, S168	C^{1486}GC to TGC	R477 to C
S108	GG^{1934}T to GAT	G626 to D
S131, S176, S239	C^{1987}GA to TGA	R644 to TGA*
S114, S166, S170	GG^{1982}C to GAC	G642 to D
S272	C^{1951}AG to TAG	Q632 to TAG*
S292	C^{1924}AA to TAA	Q623 to TAA*

* Nonsense mutation

Table S1. Four genes with mutations in suppressor strain S37

Gene ID	Nucleotide mutation	Amino acid change
FGSG_04322	GAC^{1449} to GAT	Synonymous (no change at D483)
FGSG_05186	Insertion of C after A^{206}	Frameshift after Y69
FGSG_06279	Duplication of CGTCTCAAGAAGATCGAGGA CGAGAAG (1807-1833)	Tandem duplication of RLKKIEDEK (603-611)
FGSG_09392	AA^{293}G to AGG	K98 to R

FIGURE LEGENDS

Fig. 1. Suppression of the *Fgprp4* mutant by a tandem duplication in *FgSNU66*.

A. Schematic drawing of FgSnu66 and the position of R^{603}LKKIEDEK^{611} that was duplicated in suppressor S37. HIND: Hub1-interacting domain (3-21 aa). **B.** Three-day-old PDA plates and 14-dpf mating cultures of the wild-type strain PH-1, *Fgprp4* mutant, suppressor strain S37, and *Fgprp4 FgSNU66*^{9aaD} transformant. Arrows point to ascospore cirrhi oozed out from black perithecia. **C.** Drop-inoculated wheat heads of cultivar Xiaoyan 22 were photographed 14 days post-inoculation (dpi). Black dots mark the inoculated spikelets.

Fig. 2. Intron splicing efficiency in suppressor strain S37.

A. Box-plots of intron retention levels in PH-1, *Fgprp4* mutant, and suppressor strain S37. The statistical significance for each comparison by t-test (P<0.0001) was labelled on the top. **B.** Intron splicing in the marked genes were verified by RT-PCR with primers flanking the introns with reduced splicing efficiency (marked with *). Lanes 1-4 were PCR products amplified from genomic DNA of PH-1 and cDNA of PH-1, *Fgprp4*, and S37, respectively. The size of amplified bands is labelled on the right.

Fig. 3. Suppressor mutations in *FgSNU66* and phenotypes of representative suppressors.

A. Schematic drawing of FgSnu66 and sequence alignment of its orthologs from *F. verticillioides* (*Fv*), *F. oxysporum* (*Fo*), *N. crassa* (*Nc*), *M. oryzae* (*Mo*), and *S. pombe* (*Sp*) in the marked regions. Suppressor mutations at specific sites (boxed) were labelled on the top. **B.** Wheat

heads of cultivar Xiaoyan 22 were inoculated with conidia of the marked strains and photographed at 14 dpi. Black dots mark the inoculation sites. **C.** Corn silks inoculated with culture blocks of the labelled strains were examined at 5 dpi. **D.** Three-day-old PDA cultures of PH-1, S60, S92, S131, T131, and S221. **E.** Perithecia formed by PH-1, S60, S108, S131, T131, and S292 were examined for ascosporogenous tissues at 14 dpf. Bar = 20 μm.

Fig. 4. Expression and localization of FgSnu66- and FgSnu66^{R477H}-GFP fusion proteins.

A. Conidia and hyphae of the *FgSNU66*-GFP transformants were stained with DAPI and examined by DIC and epifluorescence microscopy. **B.** Conidia and 6 h germlings of the *FgSNU66*^{R477H}-GFP transformants of PH-1 (wild type) and suppressor S37 (*Fgprp4 FgSNU66*^{9aaD}). The R477H mutation and deletion of *FgPRP4* had no effect on the subcellular localization of FgSnu66. Bars = 10 μm.

Fig. 5. Suppression of *Fgprp4* by deletion of C-terminal 27 aa (CT27) region of *FgSNU66*.

A. Three-day-old PDA cultures of PH-1 and the *Fgprp4 FgSNU66*$^{\Delta CT27}$ transformant (ΔCT27). **B.** Perithecia and ascospore cirrhi formed by mating cultures at 10 dpf. **C**. Wheat heads inoculated with the labelled strains were photographed at 14 dpi. Black dots mark the inoculated spikelets.

Fig. 6. Assays for the role of C-terminal 24 aa (CT24) in the interaction of FgSnu66 with other tri-snRNP proteins.

A. Yeast two-hybrid assays for the interaction of FgSnu66^{WT} or FgSnu66$^{\Delta CT24}$ (bait) with FgPrp8-3, FgPrp8-5, FgPrp6, and FgHub1 (Prey). FgPrp8-3 **(**1213-1789 aa) containing the Thumb/X and endonuclease domains and FgPrp8-5 **(**2101-2370 aa) containing the Jab1/MPN domain. Different concentrations (cells ml^{-1}) of the labelled yeast transformants were assayed for growth on SD-Trp-Leu-His plates. The positive (P) and negative (N) controls were provided in the BD Matchmaker library construct kit. **B.** Quantitative assays for LacZ activities with ONPG as the substrate. Mean and standard error were calculated from three independent replicates. Marker * indicates statistically significant differences (P= 0.05).

Fig. 7. Phosphorylation of FgSnu66 at T418A S420A S422A is important for plant infection.

A. Sequence alignment of the 416-455 aa region of FgSnu66 with its orthologs from *Fusarium verticillioides* (*Fv*), *Fo, F. oxysporum* (*Fo*), *Magnaporthe oryzae* (*Mo*), *Podospora anserine* (*Pa*), *Neurospora crassa* (*Nc*). The phosphorylation sites identified by MALDI-TOF/TOF MS analysis in FgSnu66 were marked with the letter P on the top. **B.** Three-day-old PDA cultures of PH-1, *Fgprp4* mutant (FP1), and the *Fgprp4 FgSNU66*$^{T418A\ S420A\ S422A}$-GFP (TSS-1) or *Fgprp4 FgSNU66*$^{T445A\ S446A}$-GFP (TS-2) transformant. **C.** Asci and ascospores of PH-1 and the TSS-1 and TS-2 transformants. Bar = 20 μm. **D.** Wheat coleoptiles and corn silks inoculated with PH-1 and the TSS-1 and TS-2 transformants were photographed at 7 and 5 dpi, respectively. Lengths of corn silks lesions were measured. Mean and standard deviation were calculated from three independent experiments. Different letters indicate statistically significant differences (P= 0.05).

Fig. 8. A putative model for the function of the C-terminal tail of FgSnu66.

FgSnu66 has an N-terminal HIND domain that may be involved in its interaction with FgHub1. At the C-terminus, FgSnu66 is 27-aa longer than its yeast ortholog, which has a C-terminal globular domain for interacting with Prp8 and Prp6. The C-terminal tail region of FgSnu66 may facilitate its interaction with FgHub1 via the HIND domain but interfere with its interaction with FgPrp8 and FgPrp6 via the putative globular domain (PGD). Phosphorylation of FgSnu66 by FgPrp4 and suppressors mutations identified in this study may reduce or abolish the negative effect of the C-terminal tail on the interaction of PGD with FgPrp8 and FgPrp6.

SUPPORTING INFORMATION

Table S1. Mutations identified in four predicted genes in suppressor strain S37.

Table S2. Phosphorylation sites in FgSnu66 identified by MALDI-TOF/TOF MS analysis.

Table S3. Primers used in this study.

Fig. S1. Generation of the *FgSnu66*^{9aaD}, *FgSnu66*^{R644*}, and *FgSnu66*$^{\Delta CT27}$ transformants.

A. The *FgSNU66*^{9aaD} gene replacement construct and recombination events.

B. The *FgSNU66*^{R644*} gene replacement construct and recombination events.

C. The *FgSNU66*$^{\Delta CT27}$ gene replacement construct and recombination events.

The directions and names of the primers used to generate the gene replacement constructs and screen for mutants were marked. The geneticin resistance cassette (Gen^{R}) was amplified from plasmid vector pFL2.

Fig. S2. The phenotypes of *FgSNU66*^{9aaD} transformants.

A. Three-day-old PDA cultures of the wild-type strain PH-1 and *FgSNU66*^{9aaD} transformants (9D08 and 9D10).

B. Mating cultures of the same set of strains were examined 8 days post-fertilization.

C. Corn silks infected with PH-1 and *FgSNU66*^{9aaD} transformants were examined at 5 dpi.

Fig. S3. Schematic draw of the *FgSNU66* and *FgHUB1* gene replacement constructs.

A. Primers 79-1F, 79-2R, 79-3F, and 79-4R were used to generate the *FgSNU66* (FGSG_06279) gene replacement construct. The 79-5F, 79-6R, H850, and H852 primers were used for PCR screen.

B. Primers 42-1F, 42-2R, 42-3F, and 42-4R were used to generate the *FgHUB1* (FGSG_09442) gene replacement construct. The 42-5F, 42-6R, H850, and H852 primers were used for PCR screen.

Fig. S4. Co-IP assays of the intra-molecular interaction of FgSnu66.

Immunoblots of total proteins (Total) and proteins eluted from anti-GFP beads (Elution) from transformants expressing the FgSnu66^{N596}-GFP and FgSnu66^{CT50}-3xFLAG fusion constructs were detected with the anti-FLAG, anti-GFP, and anti-GAPDH antibodies. Proteins eluted from anti-GFP beads (elution) of the wild-type strain PH-1 were included as the control. The expected sizes of protein bands were labelled on the right.

Fig. S5. Yeast two-hybrid assays for the interaction between FgSnu66 and FgBrr2.

Different concentrations (cells ml^{-1}) of yeast cells expressing the FgSnu66$^{\Delta CT24}$ or FgSnu66^{WT} bait construct and FgBrr2N (1-872 aa) or FgBrr2C (1285-2206 aa) prey construct were assayed for growth on SD-Trp-Leu-His plates. The positive (P) and negative (N) controls were provided in the BD Matchmaker library construct kit.

Fig. S6. Schematic drawing of the possible unequal crossing over event between the flanking GAGAAGCG sequences giving rise to the duplication of nine amino acids (EKRLKKIED).

REFERENCES

Agafonov, D.E., B. Kastner, O. Dybkov, R.V. Hofele, W.T. Liu, H. Urlaub, R. Lührmann & H. Stark, (2016) Molecular architecture of the human U4/U6•U5 tri-snRNP. *Science* **351**: 1416-1420.

Bai, G. & G. Shaner, (1994) Scab of wheat: prospects for control. *Plant Dis* **78**: 760-766.

Bai, G. & G. Shaner, (2004) Management and resistance in wheat and barley to Fusarium head blight. *Annu Rev Phytopathol* **42**: 135-161.

Boesler, C., N. Rigo, D.E. Agafonov, B. Kastner, H. Urlaub, C.L. Will & R. Lührmann, (2015) Stable tri-snRNP integration is accompanied by a major structural rearrangement of the spliceosome that is dependent on Prp8 interaction with the 5' splice site. *RNA* **21**: 1993-2005.

Bottner, C.A., H. Schmidt, S. Vogel, M. Michele & N.F. Käufer, (2005) Multiple genetic and biochemical interactions of Brr2, Prp8, Prp31, Prp1 and Prp4 kinase suggest a function in the control of the activation of spliceosomes in *Schizosaccharomyces pombe*. *Curr Genet* **48**: 151-161.

Bruno, K.S., F. Tenjo, L. Li, J.E. Hamer & J.R. Xu, (2004) Cellular localization and role of kinase activity of *PMK1* in *Magnaporthe grisea*. *Eukaryot Cell* **3**: 1525-1532.

Cohen, P., (2000) The regulation of protein function by multisite phosphorylation – a 25 year update. *Trends Bioch Sci* **25**: 596–601.

Colot, H.V., G. Park, G.E. Turner, C. Ringelberg, C.M. Crew, L. Litvinkova, Weiss R.L., K.A. Borkovich & J.C. Dunlap, (2006) A high-throughput gene knockout procedure for *Neurospora* reveals functions for multiple transcription factors. *Proc Natl Acad Sci U S A* **103**: 10352-10357.

Cuomo, C.A., U. Gueldener, J.R. Xu, F. Trail, B.G. Turgeon, A. Di Pietro, J.D. Walton, L.J. Ma, S.E. Baker, M. Rep, G. Adam, J. Antoniw, T. Baldwin, S. Calvo, Y.L. Chang, D. DeCaprio, L.R. Gale, S. Gnerre, R.S. Goswami, K. Hammond-Kosack, L.J. Harris, K. Hilburn, J.C. Kennell, S. Kroken, J.K. Magnuson, G. Mannhaupt, E. Mauceli, H.W. Mewes, R. Mitterbauer, G. Muehlbauer, M. Munsterkotter, D. Nelson, K. O'Donnell, T. Ouellet, W.H. Qi, H. Quesneville, M.I.G. Roncero, K.Y. Seong, I.V. Tetko, M. Urban, C. Waalwijk, T.J. Ward, J.Q. Yao, B.W. Birren & H.C. Kistler, (2007) The *Fusarium graminearum* genome reveals a link between localized polymorphism and pathogen specialization. *Science* **317**: 1400-1402.

Desjardins, A.E., (2003) *Gibberella* from A (*venaceae*) to Z (*eae*). *Annu Rev Phytopathol* **41**: 177-198.

Dittmar, G.A.G., C.R.M. Wilkinson, P.T. Jedrzejewski & D. Finley, (2002) Role of a ubiquitin-Like modification in polarized morphogenesis. *Science* **295**: 2442-2446.

Galej, W.P., C. Oubridge, A.J. Newman & K. Nagai, (2013) Crystal structure of Prp8 reveals active site cavity of the spliceosome. *Nature* **493**: 638-643.

Gao, X., Q. Jin, C. Jiang, Y. Li, C. Li, H. Liu, Z. Kang & J.R. Xu, (2016) FgPrp4 kinase is important for spliceosome B-Complex activation and splicing efficiency in *Fusarium*

graminearum. *PLoS Genet* **12**: e1005973.

Gao, X., J. Zhang, C. Song, K. Yuan, J. Wang, Q. Jin & J.R. Xu, (2018) Phosphorylation by Prp4 kinase releases the self-inhibition of FgPrp31 in *Fusarium graminearum*. *Curr Genet*.

Goswami, R.S. & H.C. Kistler, (2004) Heading for disaster: *Fusarium graminearum* on cereal crops. *Mol Plant Pathol* **5**: 515-525.

Gottschalk, A., G. Neubauer, J. Banroques, M. Mann, R. Lührmann & P. Fabrizio, (1999) Identification by mass spectrometry and functional analysis of novel proteins of the yeast [U4/U6•U5] tri-snRNP. *EMBO J* **18**: 4535-4548.

Hou, R., C. Jiang, Q. Zheng, C. Wang & J.R. Xu, (2015) The AreA transcription factor mediates the regulation of deoxynivalenol (DON) synthesis by ammonium and cyclic adenosine monophosphate (cAMP) signalling in *Fusarium graminearum*. *Mol Plant Pathol* **16**: 987-999.

Hou, Z., C. Xue, Y. Peng, T. Katan, H.C. Kistler & J.R. Xu, (2002) A mitogen-activated protein kinase gene (*MGV1*) in *Fusarium graminearum* is required for female fertility, heterokaryon formation, and plant infection. *Mol Plant Microbe Interact* **15**: 1119-1127.

Iliuk, A.B., V.A. Martin, B.M. Alicie, R.L. Geahlen & W.A. Tao, (2010) In-depth analyses of kinase-dependent tyrosine phosphoproteomes based on metal Ion-functionalized soluble nanopolymers. *Mol Cell Proteomics* **9**: 2162-2172.

Kuhn, A.N. & N.F. Käufer, (2003) Pre-mRNA splicing in *Schizosaccharomyces pombe*: regulatory role of a kinase conserved from fission yeast to mammals. *Curr Genet* **42**: 241-251.

Li, Z., I. Lee, E. Moradi, N.J. Hung, A.W. Johnson & E.M. Marcotte, (2009) Rational extension of the ribosome biogenesis pathway using network-guided genetics. *PLoS Biol* **7**: e1000213.

Liu, H., Q. Wang, Y. He, L. Chen, C. Hao, C. Jiang, Y. Li, Y. Dai, Z. Kang & J.R. Xu, (2016) Genome-wide A-to-I RNA editing in fungi independent of ADAR enzymes. *Genome Res* **26**: 499-509.

Liu, H., S. Zhang, J. Ma, Y. Dai, C. Li, X. Lyu, C. Wang & J.R. Xu, (2015) Two Cdc2 kinase genes with distinct functions in vegetative and infectious hyphae in *Fusarium graminearum*. *PLoS Pathog* **11**: e1004913.

Liu, S., R. Rauhut, H.P. Vornlocher & R. Lührmann, (2006) The network of protein-protein interactions within the human U4/U6•U5 tri-snRNP. *RNA* **12**: 1418-1430.

Liu, W., X. Zhou, G. Li, L. Li, L. Kong, C. Wang, H. Zhang & J.R. Xu, (2011) Multiple plant surface signals are sensed by different mechanisms in the rice blast fungus for appressorium formation. *PLoS Pathog* **7**: e1001261.

Lüders, J., G. Pyrowolakis & S. Jentsch, (2003) The ubiquitin-like protein HUB1 forms SDS-resistant complexes with cellular proteins in the absence of ATP. *EMBO Rep* **4**: 1169-1174.

Makarova, O.V., E.M. Makarov & R. Lührmann, (2001) The 65 and 110 kDa SR-related proteins of the U4/U6•U5 tri-snRNP are essential for the assembly of mature spliceosome. *EMBO J* **20**: 2553-2563.

Mishra, S.K., T. Ammon, G.M. Popowicz, M. Krajewski, R.J. Nagel, Ares M.Jr., T.A. Holak & S. Jentsch, (2011) Role of the ubiquitin-like protein Hub1 in splice-site usage and alternative splicing. *Nature* **474**: 173-178.

Mozaffari-Jovin, S., T. Wandersleben, K.F. Santos, C.L. Will, R. Lührmann & M.C. Wahl, (2013) Inhibition of RNA helicase Brr2 by the C-terminal tail of the spliceosomal protein Prp8. *Science* **341**: 80-84.

Nguyen, T.H., W.P. Galej, X.C. Bai, C. Oubridge, A.J. Newman, S.H. Scheres & K. Nagai, (2016) Cryo-EM structure of the yeast U4/U6•U5 tri-snRNP at 3.7 Å resolution. *Nature* **530**: 298-302.

Nguyen, T.H., W.P. Galej, X.C. Bai, C.G. Savva, A.J. Newman, S.H. Scheres & K. Nagai, (2015) The architecture of the spliceosomal U4/U6•U5 tri-snRNP. *Nature* **523**: 47-52.

Rosenberg, G.H., S.K. Alahari & N.F. Käufer, (1991) *prp4* from *Schizosaccharomyces pombe*, a mutant deficient in pre-mRNA splicing isolated using genes containing artificial introns. *Mol Gen Genet* **226**: 305-309.

Schmidt, H., K. Richert, R.A. Drakas & N.F. Käufer, (1999) *spp42*, identified as a classical suppressor of *prp4-73*, which encodes a kinase involved in pre-mRNA splicing in fission yeast, is a homologue of the splicing factor Prp8p. *Genetics* **153**: 1183-1191.

Schneider, M., H.H. Hsiao, C.L. Will, R. Giet, H. Urlaub & R. Lührmann, (2010) Human PRP4 kinase is required for stable tri-snRNP association during spliceosomal B complex formation. *Nat Struct Mol Biol* **17**: 216-221.

Sinha, R., E. Allemand, Z. Zhang, R. Karni, M.P. Myers & A.R. Krainer, (2010) Arginine methylation controls the subcellular localization and functions of the oncoprotein splicing factor SF2/ASF. *Mol Cell Biol* **30**: 2762-2774.

Stevens, S.W. & J. Abelson, (1999) Purification of the yeast U4/U6•U5 small nuclear ribonucleoprotein particle and identification of its proteins. *Proc Natl Acad Sci U S A* **96**: 7226-7231.

Stevens, S.W., I. Barta, H.Y. Ge, R.E. Moore, M.K. Young, T.D. Lee & J. Abelson, (2001) Biochemical and genetic analyses of the U5, U6, and U4/U6•U5 small nuclear ribonucleoproteins from *Saccharomyces cerevisiae*. *RNA* **7**: 1543-1553.

Trail, F., (2009) For blighted waves of grain: *Fusarium graminearum* in the postgenomics era. *Plant Physiol* **149**: 103-110.

van Nues, R.W. & J.D. Beggs, (2001) Functional contacts with a range of splicing proteins suggest a central role for Brr2p in the dynamic control of the order of events in spliceosomes of *Saccharomyces cerevisiae*. *Genetics* **157**: 1451-1467.

Wang, C., S. Zhang, R. Hou, Z. Zhao, Q. Zheng, Q. Xu, D. Zheng, G. Wang, H. Liu, X. Gao, J.W. Ma, H.C. Kistler, Z. Kang & J.R. Xu, (2011) Functional analysis of the kinome of the wheat scab fungus *Fusarium graminearum*. *PLoS Pathog* **7**: e1002460.

Wilkinson, C.R., G.A. Dittmar, M.D. Ohi, P. Uetz, N. Jones & D. Finley, (2004) Ubiquitin-like protein Hub1 is required for pre-mRNA splicing and localization of an essential splicing factor in fission yeast. *Curr Biol* **14**: 2283-2288.

Will, C.L. & R. Lührmann, (2011) Spliceosome structure and function. *Cold Spring Harb*

Perspect Biol **3**: a003707.

Yan, C., J. Hang, R. Wan, M. Huang, C.C. Wong & Y. Shi, (2015) Structure of a yeast spliceosome at 3.6-angstrom resolution. *Science* **349**: 1182-1191.

Yashiroda, H. & K. Tanaka, (2004) Hub1 is an essential ubiquitin-like protein without functioning as a typical modifier in fission yeast. *Genes Cells* **9**: 1189-1197.

Yin, T., Q. Zhang, J. Wang, H. Liu, C. Wang, J.R. Xu & C. Jiang, (2018) The cyclase-associated protein FgCap1 has both protein kinase A-dependent and -independent functions during deoxynivalenol production and plant infection in *Fusarium graminearum*. *Mol Plant Pathol* **19**: 552-563.

Zhang, Y., X. Gao, M. Sun, H. Liu & J.R. Xu, (2017) The *FgSRP1* SR-protein gene is important for plant infection and pre-mRNA processing in *Fusarium graminearum*. *Environ Microbiol* **19**: 4065-4079.

Zhou, X., G. Li & J.R. Xu, (2011a) Efficient approaches for generating GFP fusion and epitope-tagging constructs in filamentous fungi. *Methods Mol Biol* **722**: 199-212.

Zhou, X., W. Liu, C. Wang, Q. Xu, Y. Wang, S. Ding & J.R. Xu, (2011b) A MADS-box transcription factor MoMcm1 is required for male fertility, microconidium production and virulence in *Magnaporthe oryzae*. *Mol Microbiol* **80**: 33-53.

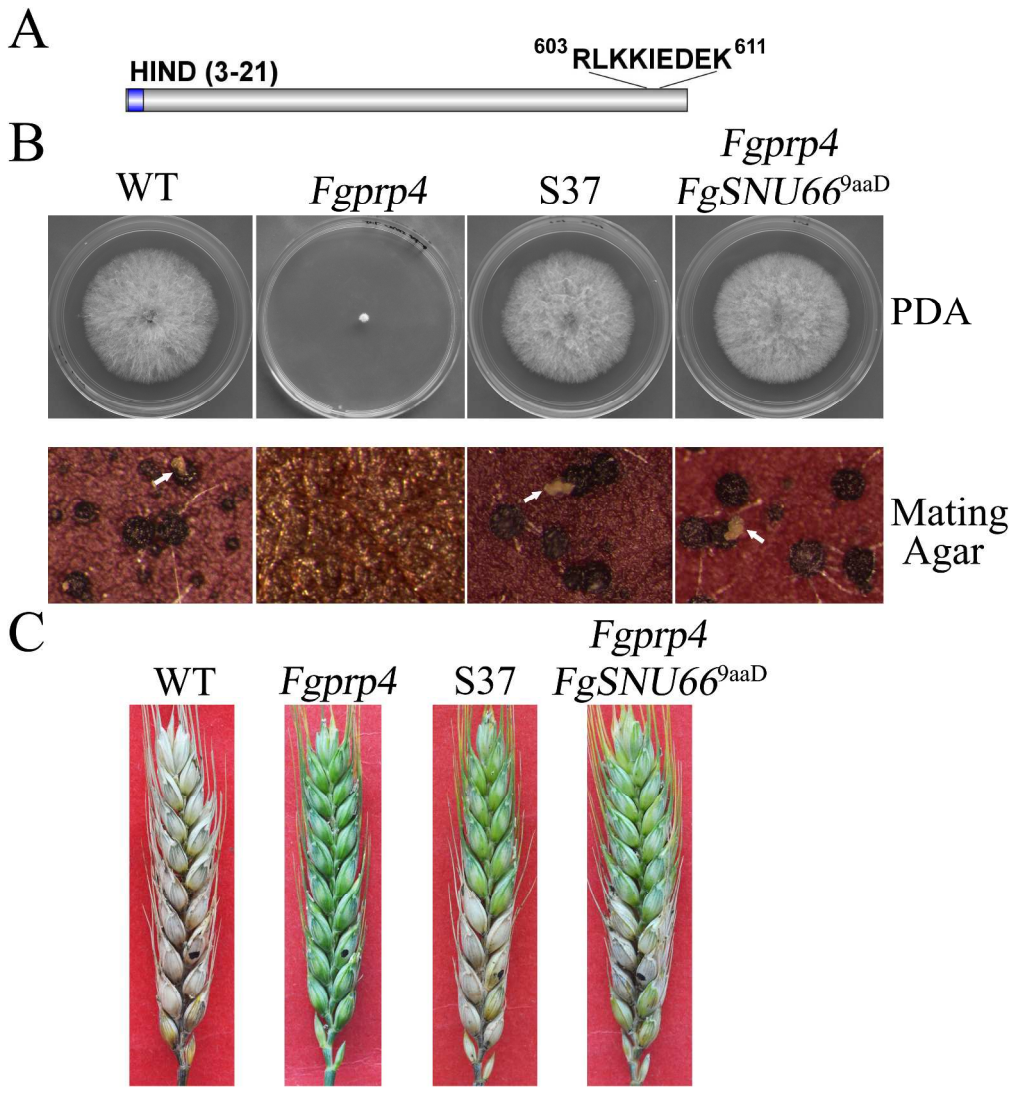

Fig. 1. Suppression of the Fgprp4 mutant by a tandem duplication in FgSNU66.
A. Schematic drawing of FgSnu66 and the position of R603LKKIEDEK611 that was duplicated in suppressor S37. HIND: Hub1-interacting domain (3-21 aa). B. Three-day-old PDA plates and 14-dpf mating cultures of the wild-type strain PH-1, Fgprp4 mutant, suppressor strain S37, and Fgprp4 FgSNU669aaD transformant. Arrows point to ascospore cirrhi oozed out from black perithecia. C. Drop-inoculated wheat heads of cultivar Xiaoyan 22 were photographed 14 days post-inoculation (dpi). Black dots mark the inoculated spikelets.

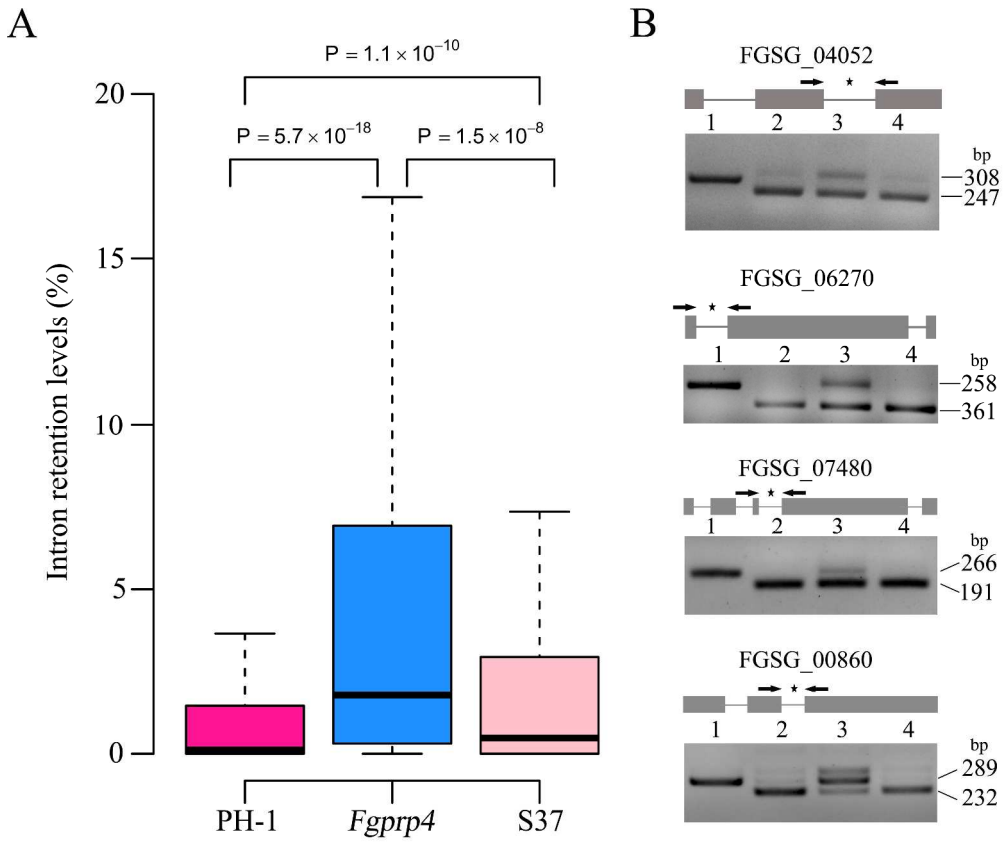

Fig. 2. Intron splicing efficiency in suppressor strain S37.
A. Box-plots of intron retention levels in PH-1, Fgprp4 mutant, and suppressor strain S37. The statistical significance for each comparison by t-test (P<0.0001) was labelled on the top. B. Intron splicing in the marked genes were verified by RT-PCR with primers flanking the introns with reduced splicing efficiency (marked with *). Lanes 1-4 were PCR products amplified from genomic DNA of PH-1 and cDNA of PH-1, Fgprp4, and S37, respectively. The size of amplified bands is labelled on the right.

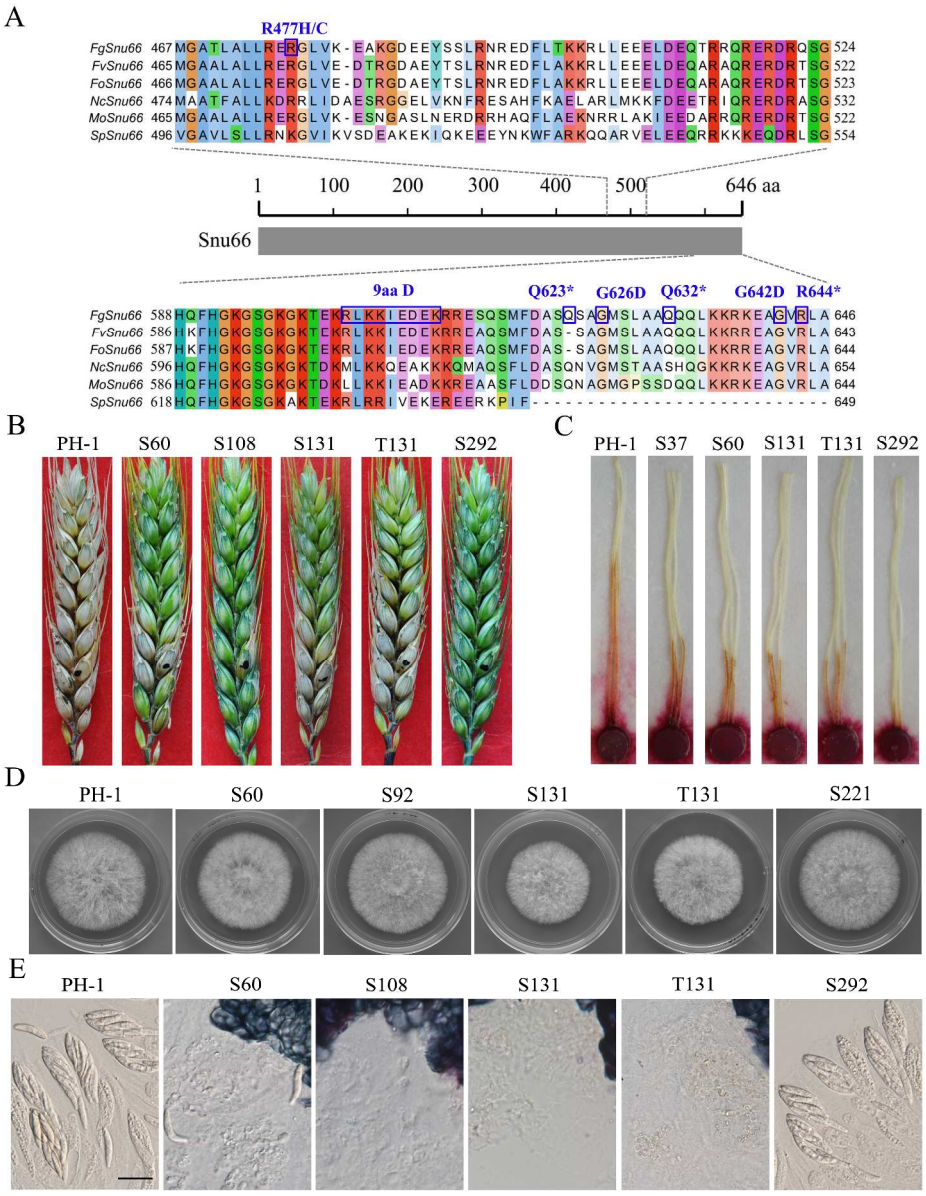

Fig. 3. Suppressor mutations in FgSNU66 and phenotypes of representative suppressors. A. Schematic drawing of FgSnu66 and sequence alignment of its orthologs from F. verticillioides (Fv), F. oxysporum (Fo), N. crassa (Nc), M. oryzae (Mo), and S. pombe (Sp) in the marked regions. Suppressor mutations at specific sites (boxed) were labelled on the top. B. Wheat heads of cultivar Xiaoyan 22 were inoculated with conidia of the marked strains and photographed at 14 dpi. Black dots mark the inoculation sites. C. Corn silks inoculated with culture blocks of the labelled strains were examined at 5 dpi. D. Three-day-old PDA cultures of PH-1, S60, S92, S131, T131, and S221. E. Perithecia formed by PH-1, S60, S108, S131, T131, and S292 were examined for ascosporogenous tissues at 14 dpf. Bar=20 μm.

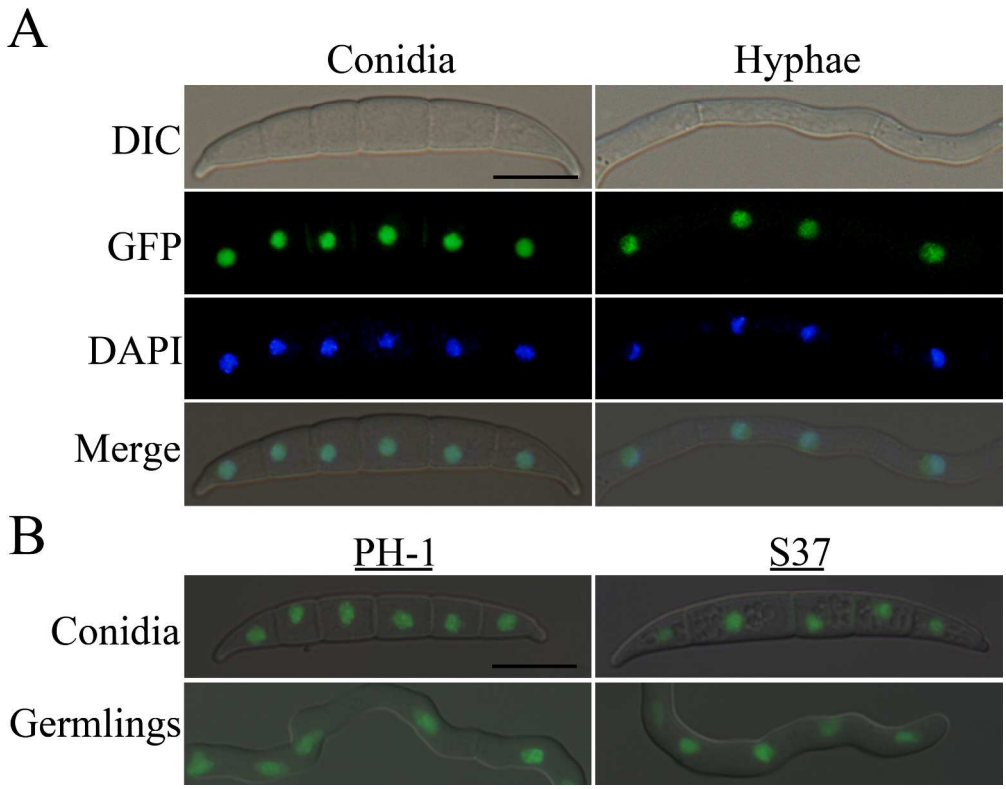

Fig. 4. Expression and localization of FgSnu66- and FgSnu66R477H-GFP fusion proteins.
A. Conidia and hyphae of the FgSNU66-GFP transformants were stained with DAPI and examined by DIC and epifluorescence microscopy. B. Conidia and 6 h germlings of the FgSNU66R477H-GFP transformants of PH-1 (wild type) and suppressor S37 (Fgprp4 FgSNU669aaD). The R477H mutation and deletion of FgPRP4 had no effect on the subcellular localization of FgSnu66. Bars = 10 μm.

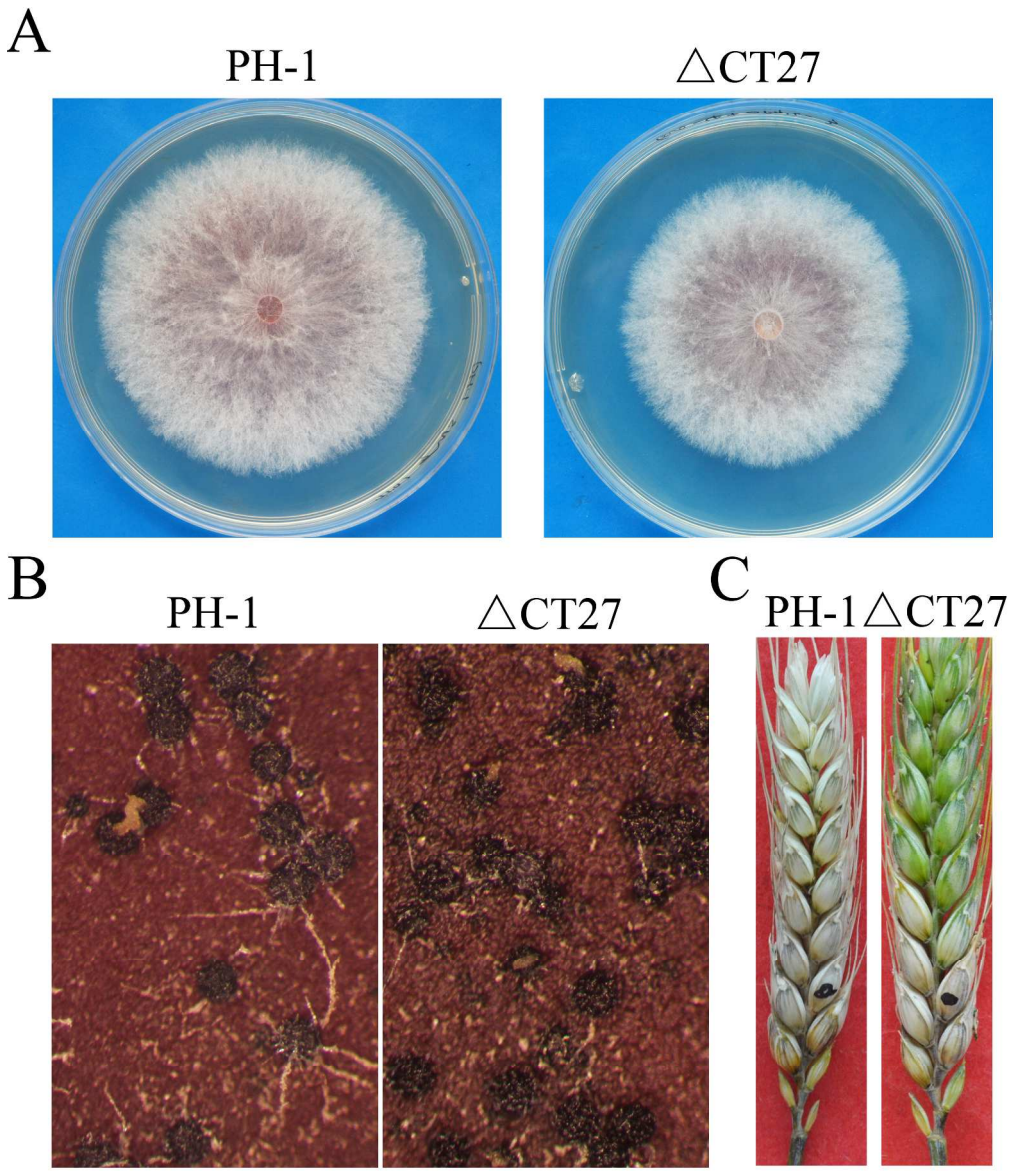

Fig. 5. Suppression of Fgprp4 by deletion of C-terminal 27 aa (CT27) region of FgSNU66.
A. Three-day-old PDA cultures of PH-1 and the Fgprp4 FgSNU66ΔCT27 transformant (ΔCT27). B. Perithecia and ascospore cirrhi formed by mating cultures at 10 dpf. C. Wheat heads inoculated with the labelled strains were photographed at 14 dpi. Black dots mark the inoculated spikelets.

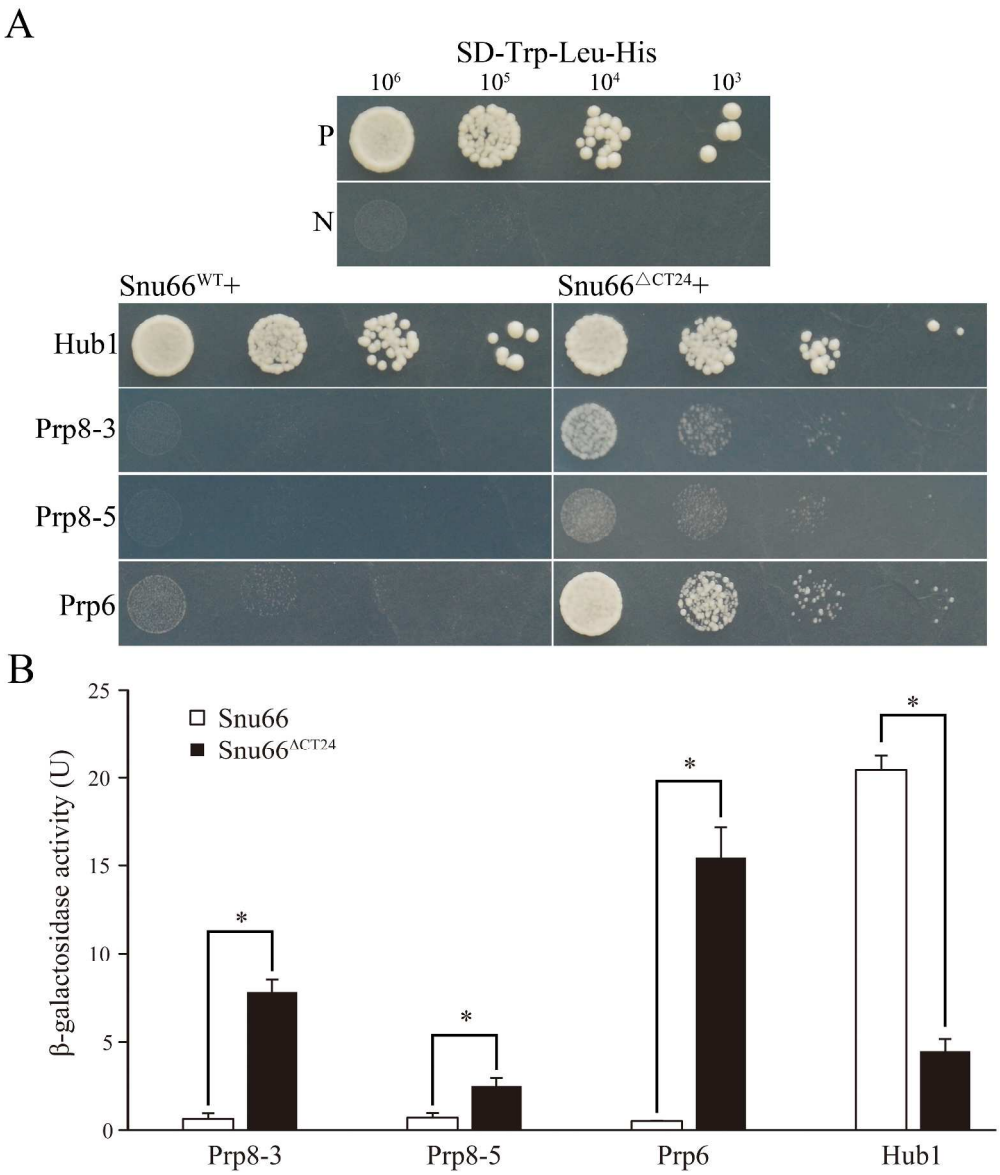

Fig. 6. Assays for the role of C-terminal 24 aa (CT24) in the interaction of FgSnu66 with other tri-snRNP proteins.

A. Yeast two-hybrid assays for the interaction of FgSnu66WT or FgSnu66ΔCT24 (bait) with FgPrp8-3, FgPrp8-5, FgPrp6, and FgHub1 (Prey). FgPrp8-3 (1213-1789 aa) containing the Thumb/X and endonuclease domains and FgPrp8-5 (2101-2370 aa) containing the Jab1/MPN domain. Different concentrations (cells ml-1) of the labelled yeast transformants were assayed for growth on SD-Trp-Leu-His plates. The positive (P) and negative (N) controls were provided in the BD Matchmaker library construct kit. B. Quantitative assays for LacZ activities with ONPG as the substrate. Mean and standard error were calculated from three independent replicates. Marker * indicates statistically significant differences (p= 0.05).

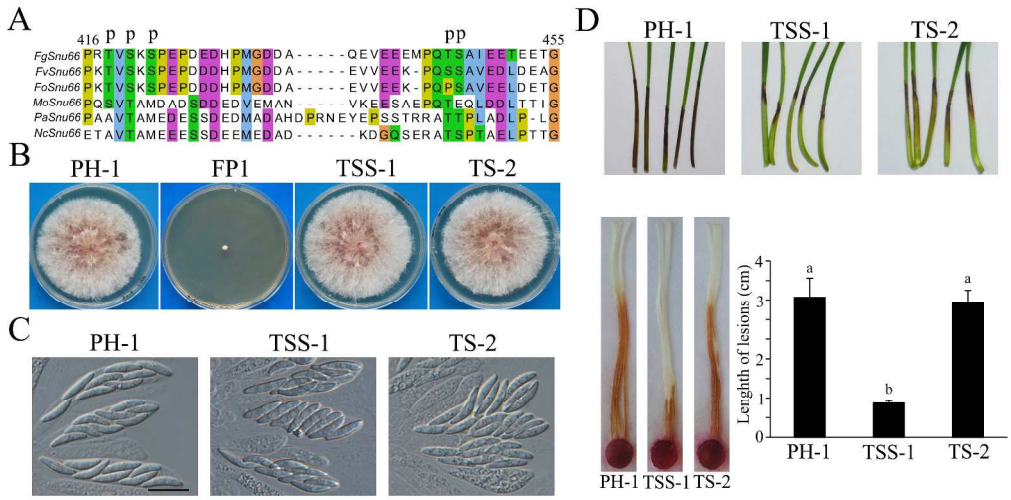

Fig. 7. Phosphorylation of FgSnu66 at T418A S420A S422A is important for plant infection. A. Sequence alignment of the 416-455 aa region of FgSnu66 with its orthologs from Fusarium verticillioides (Fv), Fo, F. oxysporum (Fo), Magnaporthe oryzae (Mo), Podospora anserine (Pa), Neurospora crassa (Nc). The phosphorylation sites identified by MALDI-TOF/TOF MS analysis in FgSnu66 were marked with the letter P on the top. B. Three-day-old PDA cultures of PH-1, Fgprp4 mutant (FP1), and the Fgprp4 FgSNU66T418A S420A S422A-GFP (TSS-1) or Fgprp4 FgSNU66T445A S446A-GFP (TS-2) transformant. C. Asci and ascospores of PH-1 and the TSS-1 and TS-2 transformants. Bar = 20 μm. D. Wheat coleoptiles and corn silks inoculated with PH-1 and the TSS-1 and TS-2 transformants were photographed at 7 and 5 dpi, respectively. Lengths of corn silks lesions were measured. Mean and standard deviation were calculated from three independent experiments. Different letters indicate statistically significant differences (p= 0.05).

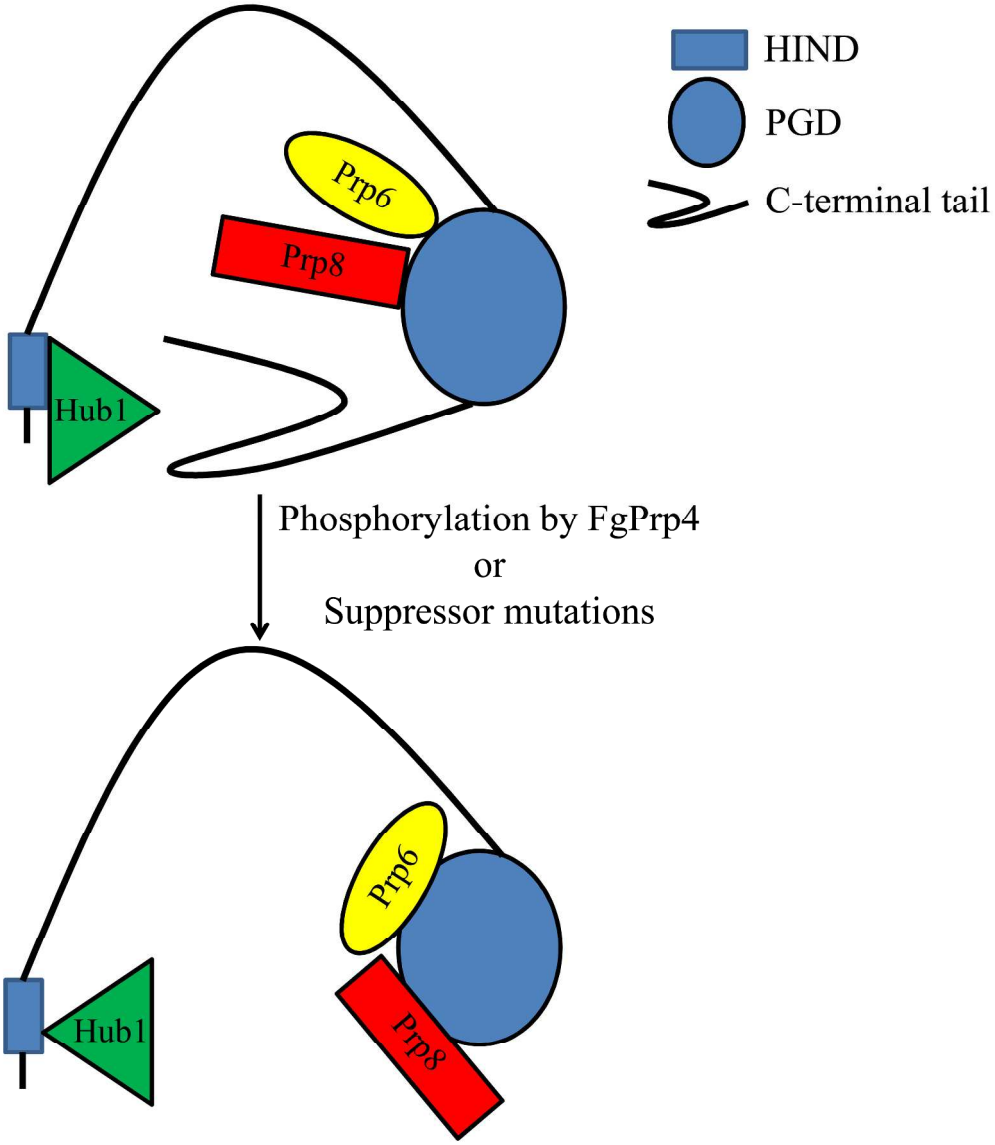

Fig. 8. A putative model for the function of the C-terminal tail of FgSnu66.
FgSnu66 has an N-terminal HIND domain that may be involved in its interaction with FgHub1. At the C-terminus, FgSnu66 is 27-aa longer than its yeast ortholog, which has a C-terminal globular domain for interacting with Prp8 and Prp6. The C-terminal tail region of FgSnu66 may facilitate its interaction with FgHub1 via the HIND domain but interfere with its interaction with FgPrp8 and FgPrp6 via the putative globular domain (PGD). Phosphorylation of FgSnu66 by FgPrp4 and suppressors mutations identified in this study may reduce or abolish the negative effect of the C-terminal tail on the interaction of PGD with FgPrp8 and FgPrp6.

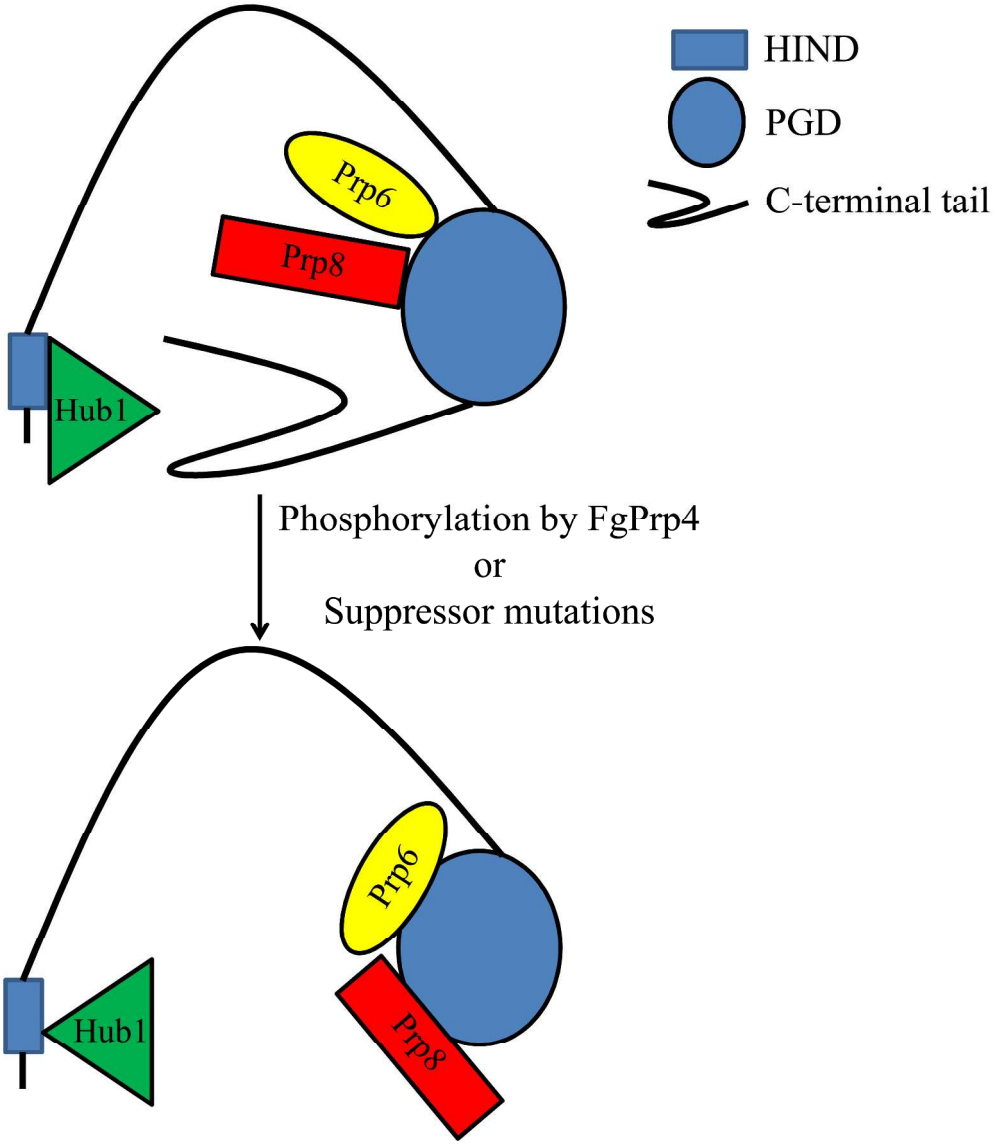

Phosphorylation of FgSnu66 by FgPrp4 or suppressor mutations identified in this study likely relieve the self-inhibitory bindings its C-terminal tail with the N-terminal region, which in turn enhance its interaction with Prp6 and Prp8 for spliceosome activation.